REPORT DOCUMENTATION PAGE

AFRL-SR-BL-TR-01- 0399

8

1. AGENCY USE ONLY *(Leave blank)*	2. REPORT DATE	3. REPORT TYPE AND DATES COVERED
	JUNE 2001	FINAL TECHNICAL REPORT 15 Nov 97 - 14 Jan 01

4. TITLE AND SUBTITLE
ACCURACY AND APPLICATION OF DOPPLER GLOBAL VELOCIMETRY TO COMPLEX AERODYNAMIC FLOWS

5. FUNDING NUMBERS
F49620-98-1-0068

3484/BS
61103D

6. AUTHOR(S)
JOHN M. KUHLMAN

7. PERFORMING ORGANIZATION NAME(S) AND ADDRESS(ES)
WEST VIRGINIA UNIVERSITY
MECHANICAL AND AEROSPACE ENGINEERING DEPT
MORGANTOWN, WV 26506-6106

8. PERFORMING ORGANIZATION REPORT NUMBER

9. SPONSORING/MONITORING AGENCY NAME(S) AND ADDRESS(ES)
AIR FORCE OFFICE OF SCIENTIFIC RESEARCH
801 N. RANDOLPH STREET, ROOM 732
ARLINGTON, VA 22203-1977

10. SPONSORING/MONITORING AGENCY REPORT NUMBER

11. SUPPLEMENTARY NOTES

20010712 016

12a. DISTRIBUTION AVAILABILITY STATEMENT
APPROVED FOR PUBLIC RELEASE, DISTRIBUTION IS UNLIMITED

12b. DISTRIBUTION CODE

13. ABSTRACT *(Maximum 200 words)*

A TWO-COMPONENT POINT Doppler velocimeter system using iodine vapor absorption cells has been improved through the use of vapor-limited cells that are insensitive to temperature variations. Also, use of a measurement volume of reduced size has improved the RMS results. Two-component velocity measurements have been obtained for a 1 inch diameter uniform circular jet flow at a nominal exit velocity of 60 m/sec, corresponding to a Reynolds number of 100,000. Similar data have also been obtained for an annular jet and a swirling jet. These data runs have been duplicated to judge the repeatability of these measurements, and also have been compared with single-component hot wire anemometer data for the same flow conditions. Mean velocity results are repeatable to within approximately 1-2 m/sec; the RMS velocity results are repeatable to within approximately 1 m/sec. Exit profiles of mean axial velocity data generally agree with hot wire anemometer results to within about 2-4 m/sec. However, the RMS velocity results are consistently 20-28% lower than the hot wire results everywhere but at the exit of the standard jet, where they are too high relative to the hot wire data. This is believed to be due to spatial averaging for the point Doppler velocimeter results, as well as to the method used to compute the RMS for some of these results. The two-component Doppler Global Velocimeter (DGV) system has also been significantly improved in the present work through the use of the sam vapor-limited iodine cells that are not sensitive to temperature variations.

14. SUBJECT TERMS

15. NUMBER OF PAGES
33

16. PRICE CODE

17. SECURITY CLASSIFICATION OF REPORT	18. SECURITY CLASSIFICATION OF THIS PAGE	19. SECURITY CLASSIFICATION OF ABSTRACT	20. LIMITATION OF ABSTRACT
U	U	U	

ACCURACY AND APPLICATION OF DOPPLER GLOBAL VELOCIMETRY TO COMPLEX AERODYNAMIC FLOWS

Final Report

AFOSR/DEPSCoR Grant F49620-98-1-0068

John M. Kuhlman, PI
West Virginia University
Mechanical and Aerospace Engineering Department
Morgantown, WV 26506-6106

Abstract

A two-component point Doppler velocimeter system using iodine vapor absorption cells has been improved through the use of vapor-limited cells that are insensitive to temperature variations. Also, use of a measurement volume of reduced size has improved the RMS results. Two-component velocity measurements have been obtained for a 1 inch diameter uniform circular jet flow at a nominal exit velocity of 60 m/sec, corresponding to a Reynolds number of 100,000. Similar data have also been obtained for an annular jet and a swirling jet. These data runs have been duplicated to judge the repeatability of these measurements, and also have been compared with single-component hot wire anemometer data for the same flow conditions. Mean velocity results are repeatable to within approximately 1-2 m/sec; the RMS velocity results are repeatable to within approximately 1 m/sec. Exit profiles of mean axial velocity data generally agree with hot wire anemometer results to within about 2-4 m/sec. However, the RMS velocity results are consistently 20-28% lower than the hot wire results everywhere but at the exit of the standard jet, where they are too high relative to the hot wire data. This is believed to be due to spatial averaging for the point Doppler velocimeter results, as well as to the method used to compute the RMS for some of these results.

The two-component Doppler Global Velocimeter (DGV) system has also been significantly improved in the present work through the use of the same vapor-limited iodine cells that are not sensitive to temperature variations. Two-component DGV velocity measurements have been obtained for the 1 inch diameter uniform circular jet flow at a nominal exit velocity of 60 m/sec. DGV mean velocity results using the vapor-limited iodine cells are repeatable to within approximately 1-3 m/sec; this is comparable to the repeatability of the point Doppler velocimeter mean velocity results.

Introduction

Several different non-intrusive whole field velocimetry techniques are currently under development that provide velocity data in a plane, which can thus reduce the time required to map out a complex flow field. Doppler Global Velocimetry (DGV), also known as Planar Doppler Velocimetry (PDV), is one such nonintrusive, planar imaging, Doppler-based velocimetry technique. The feasibility of DGV for velocity measurement was first demonstrated by Komine, et. al. in 1991 [1]. The present work investigates the accuracy of DGV, as well as related point Doppler velocimetry. Both of these techniques use a heated, temperature-controlled glass cell filled with molecular iodine vapor to measure the Doppler shift of laser light which is scattered off of small, micron-sized seed particles in an air flow. The

three-dimensional velocity field can be reconstructed in a flow by obtaining measurements from three different viewing directions. Molecular iodine vapor exhibits absorption lines that overlap the green (514.5 nm) wavelength of an Argon ion laser. Other absorption lines overlap the 532 nm wavelength of a frequency-doubled pulsed Nd:YAG laser. The laser beam is spread into a two-dimensional laser light sheet that illuminates a planar region of the flow of interest. This region is then viewed through the iodine cell by a video camera (in DGV) or photodetector (in point Doppler velocimetry) that is used to record the data. The amount of light transmitted through the cell varies as the frequency of the scattered light changes. Regions of different velocity result in different Doppler frequency shifts for this scattered light, which result in different intensities of the light transmitted through the cell. To compensate for variations in light intensity across the field of view and spatial variations in the amount of seeding material, the same region is viewed by a second detector that does not image through the iodine cell, so that the ratio of signal-to-reference detector signals is proportional to the Doppler frequency shift and velocity.

DGV velocity measurement technology has several advantages over existing sensors. First, it does not significantly alter the flow patterns being measured, as do pitot or hot wire probes. Second, since velocity data are obtained in a planar imaging region, DGV data can be acquired in less time than is required for scanning a point measurement technique such as pitot or hot wire probes, or conventional Laser Velocimetry (LV). This greatly reduces the cost of obtaining such measurements, especially in large wind tunnels. Also, DGV should allow the development of greater insight into the physical behavior of complex flows. Third, DGV is not limited to the measurement of the velocity components in the plane of the laser illumination, as is conventional particle image velocimetry (PIV). Fourth, DGV does not require resolving the motion of individual seed particles, as is the case for PIV; this is beneficial in large facilities. Fifth, DGV has advantages over PIV for the measurement of velocities at high Mach numbers. Finally, DGV also usually offers the best available spatial resolution, again, especially in large scale flow facilities. On the other hand, PIV is clearly superior in applications at low velocities, since the minimum velocity resolution for DGV is typically no better than 0.5-1 m/sec. Also, PIV has, to date, demonstrated somewhat better percent accuracy than DGV.

Point Doppler velocimetry technology is a related technique, where the video cameras are replaced by photodiodes, along with a pair of front lenses and a pinhole, to collect scattered light from a single point in a flow. Once fully developed, this technique may be an attractive alternative to LV, since it is both nonintrusive, as well as being capable of the continuous signal and high data rates typical of hot wire anemometry. This allows the use of well-developed signal processing algorithms for equally-spaced time series data for the calculation of spectra and correlation coefficients.

The WVU DGV research group has been concentrating on carefully documenting the achievable accuracy for typical DGV and point Doppler velocimeter systems. Dominant error sources are being determined, and system improvements are being implemented to increase accuracy. This is being done by measuring the velocity fields in simple, known flows such as fully developed turbulent pipe flow, jet flows, and a turbulent flow over an airfoil. Also, a simple rotating disk has been used as a velocity standard. Results obtained for the rotating disk using the WVU point Doppler velocimeter system gave accuracies of total measurement range on the order of 1-2% of full scale (0.5-1 m/sec) over a velocity range of approximately 60 m/sec [2]. Wheel velocity results for the WVU DGV system were accurate to between 3-6% of full scale (1.5-3 m/sec) over the same velocity range [3]. However, a time-varying mean velocity offset error was observed for all of these earlier DGV and point Doppler velocimeter results that

was as large as 8 m/sec, but usually between 2-5 m/sec. It has been found that the major cause of this error was the randomly varying stem temperatures of the iodine cells used for these measurements [4]. Since these early cells contained both solid and vapor iodine, a stem temperature variation with an RMS of as little as ±0.1°C would result in the observed velocity offset error, by changing the cell response. For the present work, these cells have been replaced by vapor-limited cells that contain only iodine vapor when at operating temperature. The goals of the present work are: 1.) to study the accuracy of the DGV and point Doppler velocimeter instruments fitted with new vapor-limited iodine cells to significantly reduce the earlier mean velocity offset error, and 2.) to study the utility and accuracy of the point Doppler system for the measurement of turbulent flow. A study of the applicability of point Doppler velocimetry to turbulent flow measurements for the flow over a NACA 0012 airfoil has been described by Webb [5] and Kuhlman and Webb [6], although these data were obtained before the vapor - limited iodine cells were received. The WVU DGV and point Doppler velocimetry work has been cited in a recent survey of the state of the art in DGV capability by Elliott and Beutner [7].

Point Doppler Velocimeter Apparatus and Procedure

The present point Doppler velocimeter system has been patterned after the basic DGV technology originally developed by Meyers, et. al. [8], in an effort to document the accuracy that is attainable with such systems. The original system hardware and software have been described in detail in [2] and in the theses by James [9] and Webb [5]. Improvements to this system for the present work include the use of vapor-limited iodine cells, the use of smaller pinholes in the spatial filters, and the focusing of the laser beam to a smaller volume, also to improve spatial resolution. Overall configuration geometry for the present jet flow measurements is shown in Fig. 1. A large cone has been connected to a blower to exhaust the seeded flow from the laboratory. One measurement component has been configured in forward scatter, and is primarily sensitive to the jet axial velocity, while the other component has been operated in backscatter and primarily senses the jet circumferential velocity. As a result, the backscatter channel signal strength is only about 10 % as large as the forward scatter signal. The speed of the blower that feeds the jet flow apparatus has been adjusted to balance the jet flow rate and entrainment with the maximum exhaust blower flow rate. This yielded a nominal centerline exit velocity of 60 m/sec based on pitot-static probe data, corresponding to an exit Reynolds number of 100,000 based on the jet exit diameter.

Point Doppler Velocimeter System

An iodine cell has been used to monitor laser frequency drift. This laser frequency monitoring system is shown in Fig. 2. The present vapor-limited iodine cells are 3" in diameter, with a 5" optical path length. They contain only vapor phase iodine when operated at or above their filling temperature of 43 °C, and have been supplied by Innovative Scientific Systems, Inc. (ISSI), of Dayton, OH. Cell design has been patterned after the vapor-limited iodine cells used by Elliott [10,11]. These cells have been operated at a body temperature of 80 °C. Long term drift in iodine cell stem temperature has been measured to be on the order of ± 0.1-0.2 °C, once the cells have warmed up to the steady operating temperature, and short-term stem temperature fluctuations have an RMS of 0.1 °C or less. Neutral density filters and a beam expander are used to ensure that the iodine cell of the laser frequency monitoring system is not saturated by the reference beam. The laser used is a Coherent Innova 305 argon ion laser fitted with an

etalon for single mode operation, delivering approximately 1W of single frequency light at 514.5 nm. A laser spectrum analyzer has been used to monitor laser mode shape and to detect the occurrence of mode hops.

Data acquisition and data reduction software has been developed in Visual Basic 4.0; see [9,12, and 5] for details. An 8 channel, 16 bit, simultaneous-sample-and-hold IOTech model ADC488-16 A/D board is used for digital data acquisition of the photodetector output voltages for the laser frequency monitoring system, as well as for the point Doppler velocimeter velocity measuring system voltages. The RMS noise level for this board is ± 0.3 mV on a 10 volt scale.

Fig. 3 shows one of the two point Doppler velocimeter channels. Photodiodes, along with front lenses and pinholes, are used to collect scattered light from a single point in a seeded flow. Kuhlman, et. al. [2] and James [9] have described the original system in detail. For the present work, the original photodetectors have been replaced by Thor Labs PDA55 photodiodes, which have five different selectable, fixed amplifier gains. These photodiodes have less noise and less DC offset than those used previously. Also, the original beamsplitters have been replaced by custom Melles Griot "polarization-insensitive" beamsplitters (specified as uniform versus polarization axis to ± 3% at 45°). Polarizing filters have been placed in front of the beam splitters and front lenses to minimize effects due to any residual polarization sensitivity of the beam splitters. Calibration of the three iodine cells has been accomplished in situ, with the cells installed ready for data acquisition, using a continuous scan of the mode structure of the cw Argon ion laser by mechanically altering the tilt of the etalon through about 10-20 mode hops [9]. Light is scattered off of the same smoke particles that are used in the actual jet flow, but at a much lower air velocity (~1-2 m/sec). An example calibration data set and the Boltzmann fitting function curve fits are shown in Fig. 4.

Jet Facility

For the present work, a 1" diameter uniform axisymmetric jet flow facility has been utilized; see Fig. 5. A jet has been chosen for the present study because it is a well-documented simple turbulent flow [13,14] with important technological applications, that can easily be made more complex through the addition of either swirl or a non-uniform exit mean velocity profile shape (annular jet; [15]). Kuhlman [16] has reported conventional LV data for the standard uniform exit velocity jet and the annular jet. Hussain, et. al. [17] have compared LV and hot wire data in a standard jet, and found significant errors in hot wire data, but these were confined to the edges of such a jet flow, where flow reversals occur. The present jet is fed from a plenum fitted with a flow-straightening element, via a 16:1 area ratio nozzle. This nozzle has been fitted with an annular centerbody (Fig. 6) to create the annular jet with a low axial velocity on the centerline at the exit [15] or with a swirler to create a swirling jet having an exit swirl number of approximately 0.33. The flow is driven by a variable-speed blower that can achieve exit velocities of just over 100 m/sec. For the present results, the jet has been run at an exit velocity of nominally 60 m/sec, corresponding to a Reynolds number of 100,000. Flow seeding is provided by a commercial ROSCO fog machine, which feeds a large plenum, to damp out pulsations in smoke output. This has led to improved uniformity in the signal levels over time for the present jet flow data. Also, the amount of smoke produced has been reduced by placing a diode in series with the motor that drives the fog fluid pump. This has improved the quality of data, by allowing data to be taken at lower seeding levels, thus reducing the effects of secondary scattering.

A computer-controlled, three-axis traversing system has been developed, as described in the thesis by Ramanath [18] for use in positioning the jet flow facility with respect to the fixed point

Doppler velocimeter system, so that velocity contours may be mapped out in a series of traverses across the jet flow (radial direction), or along the jet axis (axial direction). Accuracy of a single traverse move has been found to be on the order of 0.001" for typical moves in one direction over distances on the order of a few inches.

Data Acquisition

Radial and axial jet mean and RMS velocity profiles have been obtained using two different techniques. For the first method, the jet flow facility has been traversed slowly but continuously with respect to the fixed point Doppler velocimeter systems using the traverse (at a rate of 0.1"/sec radially, or 0.3"/sec axially), while continuously recording the photodiode voltages using the A/D system [19]. For this data a sampling rate of 100 Hz has been used, although significantly higher rates are possible. These "strip chart" data records have been repeated 10 times for each radial or axial profile. Average and RMS velocity results have then been obtained by computing 10-point average and RMS values for each time record, and then averaging these signals for the 10 separate traverses. Thus, each average and RMS data point presented for these results is effectively based upon a one second time average, at a sampling rate of 100 Hz. During the 0.1 second over which the signal averaging operation is performed, the traverse moved the jet flow a radial distance of 0.01", which is relatively small compared to the nominal 2-3 mm diameter of the sampling volume for the point Doppler velocimeter system. This data acquisition technique was developed prior to the installation of the new vapor-limited cells, when speed of data acquisition was extremely important. The second data acquisition technique consists of conventional velocity time records at fixed locations in the flow, taken at a sampling rate of 10 kHz, with 8k blocks of data taken at each point. Also, for this second technique, the pinholes have been reduced in size to 1 mm diameter, and the laser beam has been focused from its original 2 mm diameter, down to 0.2 mm. This has been done to reduce the effects of spatial averaging, which were partly responsible for RMS results obtained using the first method being lower than hot wire results. Two-component point Doppler velocimetry data have been obtained for the uniform exit velocity standard jet, the swirling jet, and the annular jet for centerline traverses and radial traverses at x/D = 0.25, 1, 2, (3), 4, 6, 8, 10, and 12. For each jet configuration, additional runs have been made to assess data repeatability. Also, single-component constant temperature hot wire anemometer data have been acquired for the standard jet and the swirling jet, for comparison with the point Doppler velocimetry results. These data have been acquired using a TSI IFA300, at fixed points in the flow, again at a sampling rate of 10 kHz, with 8k blocks of data taken at each point. Data taken using the first acquisition method has been presented in detail by Collins [19] and summarized previously by Kuhlman and Collins [20]. The conventional point statistics of the second method using smaller pinholes and a focused laser beam have been presented by Kuhlman and Scarberry [21], and are summarized in Kuhlman, Collins and Scarberry [22].

Point Doppler Velocimeter Results

Previous Tests

Early WVU point Doppler velocimeter data repeatability, as documented in the thesis by Ramanath [18] was poor. However, improved cell calibration procedures [9] significantly increased point Doppler velocimetry and DGV system accuracy. Both single and 2-component velocity data measured on a rotating wheel have been presented in [9] and [2] with velocity range error magnitudes of approximately ±0.6-1.2 m/sec, corresponding to 1-2% errors. Also,

the standard deviations of the actual wheel velocity data points from the least squares linear curve fits was 0.5-0.7% (0.3-0.5 m/sec). This RMS error is approximately 2-3 times smaller than has been documented by other DGV researchers. Two-component data obtained from a traverse across the exit of a fully developed pipe flow at a nominal Reynolds number of 76,000 have been presented by Kuhlman [23]. The axial mean velocities agreed well with results from a pitot-static probe survey. Turbulent velocity levels generally agreed with hot wire data of Laufer [24].

However, all of these earlier results exhibited a slow, long-term drift in the recorded value of zero mean velocity. This mean velocity "offset error" was typically on the order of 2-6 m/sec, and appeared to vary randomly with time. It has been found that this offset error was largely due to the random, uncorrelated variations in iodine cell stem temperatures [4]. This stem temperature variation has been observed to vary with a short term RMS of 0.1 °C [12]. For the original iodine cells used in the DGV and point Doppler velocimeter systems, increasing the cell stem temperature would increase the amount of vapor phase iodine in the body of the cell, thus altering the cell absorption. This has been found to correspond to an error in the computed Doppler shift frequency of 7 MHz, using the iodine absorption model of Forkey [25]. This then corresponded to a mean velocity error of from 2 to 10 m/sec, depending on the geometry and viewing direction of the system [4]. This level of velocity error is consistent with the observed mean velocity offset error for this early work.

Uniform Circular Jet Data

Examples of the 2-component point Doppler velocimeter velocity data, taken using the first of the two data acquisition methods, in the uniform circular jet are presented in Figs. 7-8. These results have been presented in [22]. Data have been obtained for lateral traverses at x/D = 0.25, 1, 2, 4, 6, 8, 10, and 12, where the measured axial mean and RMS velocities are shown. Fig. 9 presents the corresponding centerline profiles of both axial and circumferential mean and RMS velocities. A complete presentation of these results has been given by Collins [19]. Mean axial velocity profiles (Fig. 7) appear to become self-similar beyond x/D = 6. Centerline mean axial velocity (Fig. 9) shows a slight decay (approximately 4-5 m/sec) over the first 3 jet diameters, as has been seen in the jet DGV data of Thorpe, et. al. [26]. However, pitot-static and hot wire measurements in this flow do not exhibit this drop in centerline velocity, instead indicating a potential core extending about 4 diameters from the exit. It may be that the smoke seed particles cause this early centerline velocity decay, although Longmire and Eaton [27] do not see a similar decay in their study of a lightly-loaded, particle-laden circular air jet. The measured smoke particle mass loading for the present results is approximately 0.5%. Mean circumferential velocities, which should everywhere be equal to zero in this flow, display an offset that varies from 0-2 m/sec near the jet exit, to a maximum value of about 3 m/sec at large x/D [19]. This variation is speculated to either be the result of variations in secondary scattering, or to inaccuracies in the iodine cell calibration curves which might be larger at different ratio values. These data have been obtained for a ratio range for the laser frequency monitoring system of nominally 0.4-0.6, with the ratio value outside of the absorption line of 0.89. Exit RMS velocities are on the order of 1.0-1.5 m/sec; it is believed that this is actually indicative of the lowest sensitivity of the current system to velocity fluctuations. This minimum measured axial turbulence intensity of about 1.7% approaches the sensitivity to turbulence typically achievable with conventional counter-processor-based LV systems. Both of the point Doppler channels are expected to have a resolution of approximately 1 m/sec, based on an error propagation model that calculates the effects of the 0.3 - 0.4 mV RMS noise in the A/D board

used in the present work. This is consistent with the measured RMS velocity data at the jet exit. Effects of laser speckle (McKenzie [28]; Smith [29]) are not believed to be a dominant source of this RMS velocity resolution, since both the seed particle size and speckle size are on the order of one micron, while the probe volume region is between 0.2 and 2.0 mm in diameter. This would result in a SNR of from 100-1000 [29], while the present results display a SNR of between 50-60, showing that the measured A/D board noise dominates. Centerline RMS velocities (Fig. 9) increase from their exit levels of about 1 m/sec to maximum values (of about 5.5 m/sec-axial; 4.5 m/sec-circumferential) at about x/D = 6, and then slowly decay. The axial and circumferential RMS velocities for traverses at x/D = 6 and beyond are nearly equal, with the axial RMS slightly higher, as would be expected in a circular jet flow [13]. Also, the centerline axial turbulence intensity at x/D = 12 is about 19%, in reasonable agreement with previous measurements [16]. Wygnanski and Fiedler found a centerline axial turbulence intensity of 28% in the far-field self-preserving region of their jet flow (beyond about 50-70 jet diameters), indicating that the present turbulence data are not yet self-preserving.

Mean velocities exhibit a variability from a smooth curve in any one traverse profile of less than 1 m/sec at the exit, to as much as 2-3 m/sec at large x/D (Fig. 7). Variability of the corresponding computed RMS velocity profiles varies from less than 0.5 m/sec at the exit, to as much as 1.5 m/sec at x/D = 12. This decrease in the smoothness of the profiles as x/D increases is due to the increased turbulence time scales farther from the jet exit. This variability in the results is not due to any limitation in the system itself, and could be significantly reduced by increasing the averaging time for data at large x/D values. A repeat run of the standard jet has been performed on a different day, and reduced with different cell calibrations, to assess the repeatability of the present data [19]. Mean velocity data for the two runs match to within about 1-2 m/sec, and RMS data match to better than 1.0 m/sec.

It has been observed that the present data do not exhibit the drift in the zero velocity offset that had been observed with the previous iodine cells. It now appears that the dominant mean velocity error source is due to the accuracy of the iodine cell calibrations, estimated as on the order of about ±1-2 m/sec. Reducing the present results a second time using a second calibration data set taken on the same day as the one used for the presented results showed a variation in the computed mean axial velocities of 1 - 3 m/sec, with no discernable effect on the computed mean circumferential or RMS velocities [19]. This variation of the mean axial velocity is slightly larger than the observed repeatability for multiple runs. However, it was noted that the additional calibration data was visibly less smooth than the calibration data that has been used to reduce the present results. This is because the additional calibration run was performed prior to that which has been used to reduce the presented results, and it generally took some practice on a given day to perfect the technique of mechanically tilting the laser etalon to cause the mode hops in a smooth, repeatable fashion.

Annular Jet Data

Similar results for the annular jet have been presented by Collins, where again repeatability for two runs is observed to be about ±1-2 m/sec [19]. This annular jet is a more complex turbulent flow that has an exit mean axial velocity profile that displays a low velocity central core (about 30 m/sec on the centerline, versus a maximum of 55 m/sec), so that in effect the annular jet possesses both an outer jet shear layer as well as an inner "wake" type of shear layer. This leads to increased turbulence levels relative to the standard uniform jet, as well as enhanced mixing, and faster centerline velocity decay. Thus, the mean axial velocity at x/D = 12 is only about 10-12 m/sec for this annular jet, as compared to a value of about 28-30 m/sec (Fig. 9) for

the standard jet. The measured RMS velocity data result in calculated turbulence intensities of between 10-15% near the exit to 25-28% at x/D = 12. Similar behavior in the annular jet was observed for a series of single-component conventional LV data in [16].

Swirling Jet Data

Radial profiles of point Doppler velocimeter data in the swirling jet (swirl number = 0.33) are presented in Figs. 10-13, where lateral traverses at x/D = 0.25,1,2,3,4,6,8, and 12 are shown. The swirling jet is another example of a more complex turbulent flow. Fig. 14 presents the corresponding centerline profiles of mean and RMS velocities. The exit mean axial velocity profile is nearly uniform (Fig. 10), similar to the standard jet case (Fig. 7), but with a thicker outer shear layer. Mean axial velocity profiles (Fig. 10) again appear to become self-similar beyond x/D = 6. Centerline mean axial velocity (Fig. 14) begins to decay immediately beyond the exit, with no evidence of a potential core. As a result, even though both the uniform and swirling jets have exit velocities of about 58-60 m/sec, the mean axial velocity of the swirling jet has decayed to about 18-20 m/sec at x/D = 12, compared to a value of about 28-30 m/sec for the uniform jet (Fig. 9). The mean swirl velocity profile at the exit (Fig. 12) is antisymmetric, and displays a near-rigid body rotation profile near the centerline ($r/D \leq 0.2$), but then levels off to a nearly constant swirl mean velocity of ±20 m/sec until $r/D \cong 0.4$. This results in an exit swirl number for this jet of nominally 0.33, based upon the maximum swirl and axial velocities at the exit. The maximum swirl velocity for a radial profile decays rapidly along the jet axis, having decayed to a maximum of ±10 m/sec at x/D = 3 (Fig. 12), ±5 m/sec at x/D = 6, and ±1-2 m/sec at x/D = 10 and 12. Beyond x/D = 6 the measured mean swirl velocity profiles are essentially a solid body rotation for the entire radial direction measurement range. These mean circumferential velocity measurements again display offsets of between 1 m/sec at the exit to maximum values of approximately 2 m/sec for large x/D. Exit RMS velocity levels (Figs. 11, 13) are higher than for the standard uniform jet (Fig. 8), and exit axial RMS is less than swirl RMS (about 1 m/sec, versus 2 m/sec). Both RMS velocities increase versus x/D (Fig. 14), reaching peak values at about x/D = 3, and then decay slowly. Note that the swirl RMS velocities are larger than the axial RMS velocities until about x/D = 8-10; beyond this both RMS velocities appear to be approaching equal values. At x/D = 12 the centerline turbulence intensities are about 25-28%.

Thus, it is noted that x/D beyond about 8 is the region where the mean axial velocity profiles appear to be self-similar, and the axial and swirl RMS velocities appear to be nearly equal. The observed levels of variability of the mean velocity data for the axial and radial profiles are quite similar to those observed for the standard jet (Figs. 7-9). The increase from less than 1 m/sec at the exit to 1.5-3 m/sec at large x/D is again due to the increased turbulence time scales as x/D increases. Finally, it is remarked that during the data runs, it was possible to visually observe the core of the vortex on the jet axis for this swirling jet for $0 \leq x/D \leq 4$.

Point Doppler/Hot Wire Jet Data Comparisons

Comparisons between the point Doppler velocimeter and hot wire anemometer axial velocity results are shown in Figs. 15-17 for the standard jet. Point Doppler velocimeter results are shown for both the strip chart data acquisition method [19] as well as new conventional statistics data obtained using method 2 [22]. Hot wire data were taken at a sampling rate of 10 kHz, with data records of 0.8192 seconds in length. The anemometer was operated in constant temperature mode, without compensation for air temperature variations. Point Doppler velocimeter mean axial velocity results generally agree with the hot wire data to within about 2-

4 m/s at the jet exit (Fig. 15). However, the point Doppler exit profiles of RMS velocities are too high for the standard jet (Fig. 15), relative to the hot wire results. Agreement between the point Doppler velocimeter and hot wire mean axial velocity results for centerline traverses (Fig. 16) is generally not as good as is observed for the exit profiles. Disagreements as large as 6-7 m/sec are observed for the earlier results from [19], while the results using acquisition method 2 display disagreements of up to 2-4 m/sec relative to the hot wire data. Note that these more recent results [22] are more accurate in the jet potential core. As was observed for the exit profiles, the jet centerline RMS velocity results differ from the hot wire results. Note that the point Doppler velocimeter axial RMS velocity results are closer to the hot wire results for the second data acquisition method, using a 10 kHz sampling rate for 0.8192 seconds, and using a smaller pinhole with a focused laser beam to reduce the spatial averaging, relative to the data taken using the first method (Figs. 16-17). In particular, the peak centerline axial RMS is only 5.5-6 m/sec for acquisition method 1 [19], while the peak RMS for method 2 is 6.5-7 m/sec, compared to the hot wire result of about 9 m/sec. These improved RMS values are still 20-30% low relative to the hot wire data. Similar levels of agreement are seen, again for the standard jet, at x/D = 6 in Fig. 17.

Point Doppler/Hot Wire NACA 0012 Airfoil Flow Data Comparisons

Sample point Doppler velocimeter velocity data are presented for flow over the NACA 0012 airfoil at a free stream velocity of approximately 21 m/sec in Figs. 18-21, taken from reference [6]. Also shown are single-component hot wire anemometer axial velocity measurements taken at the same position, but at different times. These data have been taken at $x/c \cong 0.55$, and at a fixed z coordinate of 0.5" above the airfoil shoulder, corresponding to $z/c \cong 0.04$. Both the point Doppler velocimeter and hot wire measurements have been taken at a sampling rate of 10 kHz. A DANTEC model 55P04 single sensor probe and a TSI IFA300 constant temperature anemometer have been used to acquire the hot wire data. The hot wire probe has been calibrated against a pitot-static probe at the exit of a low-turbulence air jet. These point Doppler velocimeter data have been obtained without focusing the laser beam, so the sample volume is approximately 2 mm in diameter. Also, these data were obtained before the vapor-limited cells were acquired. PDv velocity time traces appear similar to the hot wire data, although the pDv data appear somewhat noisier [6]. The hot wire data has a 5 kHz digital filter applied, whereas this has not been done for the point Doppler velocimeter data. It has been noted that hot wire time traces obtained without the digital filter applied appear somewhat noisier than the hot wire data.

Point Doppler velocimeter statistics have been computed for data records of 1 K points with a sampling rate of 10 kHz. These relatively short time records were used to minimize the time required to acquire the point Doppler velocimeter data, in an effort to minimize the effects of drift of the iodine cell calibrations. Four point Doppler velocimeter data sets and five hot wire data sets have been shown in Figs. 18-21, to indicate the level of repeatability that is observed. Streamwise (Fig. 18) and spanwise (Fig. 19) mean point Doppler velocimeter velocities show a total variability of about 5 to 6 m/sec ($\pm$2.5-3 m/sec) for the four runs; this level of non-repeatability of mean velocity data in seeded flows is consistent with earlier DGV results by Naylor and Kuhlman [4]. Also, the point Doppler velocimeter mean streamwise velocities agree with the hot wire results to within about $\pm$ 3 m/sec, and point Doppler velocimeter mean spanwise velocity is within a total error bound of $\pm$2.5 m/sec of the correct value of zero. Again, these levels of accuracy are comparable to previous DGV observations in pipe flow and jet flow [4, 23], and are independent of the total mean velocity range. These mean

velocity errors were largely due to the observed drift in iodine cell stem temperatures, which then caused drift in the cell calibrations. Streamwise (Fig. 20) and spanwise (Fig. 21) point Doppler velocimeter RMS velocity magnitudes repeat to within a total variability of about 0.5 to 0.7 m/sec. The streamwise point Doppler velocimeter RMS velocity measurements generally agree with the hot wire results to within this range of repeatability, although streamwise point Doppler velocimeter RMS values tend to be consistently lower than hot wire data towards the leading edge of the airfoil. Calculated point Doppler velocimeter longitudinal turbulence intensities vary from about 10-15 % near the leading edge of the airfoil to about 25-30 % near the trailing edge; these results agree well with the hot wire results.

In order to further compare the point Doppler velocimeter and hot wire results, MATLAB has been used to compute both time autocorrelations and power spectra at several representative locations [6]. These results have been computed for time histories of 1 K samples, again at a sampling frequency of 10 kHz. The point Doppler velocimeter correlation coefficient agrees well with the hot wire result [6]. Both point Doppler velocimeter and hot wire signal autocorrelations decay in less than 10 msec. As is the case for the RMS velocities presented in Figs. 20 and 21, the time autocorrelations are expected to be influenced predominantly by the behavior of the low-frequency, large eddies in the flow. Power spectra, on the other hand, disagree for frequencies above about 500-600 Hz, with the point Doppler velocimeter data being significantly noisier. It is speculated that this may have been due to the relatively large (~ 2 mm dia.) probe volume for these results.

Model for Point Doppler Velocimeter Minimum Velocity Resolution

As part of a contract to Metrolaser, Inc. [30], a simple error propagation model has been developed that uses the measured RMS voltages for each of the six Thor Labs PIN photodiodes in the pDv system to predict the minimum RMS velocity resolution values for each channel of the pDv system. This error model was first presented by Kuhlman and Scarberry in reference [21]. Also presented in [30] are point Doppler velocimeter results taken in the standard jet, but using a new A/D board (National Instruments model PCI-6052E), where minimum velocity resolution was improved from 1-1.5 m/sec to 0.6-0.9 m/sec. The RMS voltages have been measured using the new National Instruments A/D board, with each of the photodetectors covered over so that no light was incident. Results were nominally 0.2 mV for each of the two photodiodes used in the LFMS, and 0.4 mV for the four photodiodes used in the two point Doppler velocimeter measurement components. Note that these noise levels are considerably higher than the 0.04 mV resolution of the new A/D board, but are comparable to the 0.3-0.4 mV noise levels of the old IOTech A/D board. These measured RMS voltages due to amplifier and photodiode noise have then been used to estimate errors in the appropriate iodine cell transmission ratio, by adding the measured RMS noise voltage to the signal photodetector voltage, and subtracting the RMS noise voltage from the reference photodetector voltage. These ratios including the noise voltages have then been propagated through the iodine cell calibration curves to get frequency errors for each iodine cell, which have then been converted to predicted velocity errors using the system geometry. This error model is far simpler than that developed by McKenzie [28], but appears to correctly predict the observed RMS velocity resolution of the current point Doppler velocimeter system, where photodetector noise is the dominant random error source.

For the new A/D board this error model predicts that the RMS point Doppler velocimeter velocities should be 0.9/0.7 m/sec, based on the measured RMS noise voltages of the existing PIN photodiode sensors, for the axial and circumferential directions, respectively, in the 60

m/sec jet flow results of reference [21]. These are close to the observed RMS velocities at 60 m/sec [21], of 0.9/0.7 m/sec. This indicates that either lower noise, and/or higher output, photodetectors will be required to achieve a lower minimum velocity resolution. Also, the same error propagation model applied to the low speed (~3 m/sec) jet flow [21] predicts that the RMS velocities measured in this flow should be 0.7/0.26 m/sec in the axial/circumferential directions, respectively. Again, this compares quite favorably with the observed RMS values of 0.8/0.26 m/sec. Note that here both the measured and predicted RMS velocity levels are significantly lower for the circumferential velocity measurements, which are primarily made by the point Doppler velocimeter channel that is oriented in backscatter. This is due to the fact that while the signal strengths for all four photodiodes are nearly equal for these measurements, the sensitivity of the backscatter component to velocity is approximately 4-5 times greater than that of the forward scatter sensors.

The error model predicts a minimum velocity resolution of between 0.15-0.25 m/sec, depending on point Doppler velocimeter system geometry, for an improvement in sensor signal-to-noise ratio (SNR) of a factor of 5-10. In an effort to achieve this potential minimum velocity resolution, the present PIN photodiodes will be replaced with avalanche photodiodes (APDs) in the near future.

Doppler Global Velocimeter Apparatus and Procedure

Doppler Global Velocimeter System

The present DGV system has also been patterned after the DGV technology originally developed by Meyers, et al. [8], in an effort to document the accuracy that is attainable with such systems. The original DGV system hardware and software have been described in more detail by Naylor and Kuhlman [4], and in the dissertation by Naylor [12]. The laser frequency monitoring system (LFMS) has already been shown in Fig. 2. The new, vapor-limited iodine cells have been supplied by Innovative Scientific Systems, Inc. (ISSI), of Dayton, OH, and are 3" in diameter, with a 5" optical path length. They contain only vapor phase iodine when operated at or above their filling temperature of 43 °C. The cell design has been patterned after the vapor-limited iodine cells used by Elliott [10, 11]. These cells have been operated at a body temperature of 80 °C. Neutral density filters and a beam expander have been used to ensure that the iodine cell of the LFMS is not saturated by the reference beam. The laser used is a Coherent Innova 305 argon ion laser fitted with an etalon for single mode operation, delivering approximately 1W of single frequency light at 514.5 nm. A laser spectrum analyzer has been used to monitor laser mode shape and to detect the occurrence of mode hops. The 8 channel, 16 bit, simultaneous-sample-and-hold IOTech model ADC488-16 A/D board has been used for digital data acquisition of the LFMS photodetector output voltages.

The original beamsplitters have been replaced by custom Melles Griot "polarization-insensitive" beamsplitters (specified as uniform versus polarization axis to ±3% at 45°). Polarizing filters have been placed in front of the beam splitters to minimize effects due to any residual polarization sensitivity. Calibration of the three iodine cells has been accomplished in situ, with the cells installed ready for data acquisition, using a continuous scan of the mode structure of the cw Argon ion laser by mechanically altering the tilt of the etalon through about 10-20 mode hops [9]. Light is scattered off of the same smoke particles as are used in the actual jet flow, but at a much lower air velocity (~1-2 m/sec).

Eight bit Hitachi KP-M1 CCD cameras and a Matrox Genesis frame grabber are being used for the two component DGV system. The forward scatter cameras have Nikon 35-135mm f3.5-4

zoom lenses mounted on C-mount adapters. The backward scatter cameras are fitted with Nikon 105mm f2.5 lenses, since the backscatter light intensity is much lower than in forward scatter. Zoom lenses were selected instead of fixed focal length lenses because of their versatility in imaging different sized areas over a wide range of distances. The penalty paid for this flexibility is an increased f-number for a given focal length relative to a fixed focal length lens. The frame grabber has four inputs, each leading to eight bit digitizers. This configuration allows all four cameras to be read simultaneously, as long as the cameras have been synchronized. The same horizontal and vertical sync signals are fed to each of the cameras by the Genesis board. Maximizing data rates for this system is not a concern since the fastest data rates possible with the cameras are still not fast enough to resolve any significant time varying flow structures. The continuous data acquisition rate, writing to the hard drive, for the two component system is approximately 2 sets of four frames/sec, while short bursts of data (10 frames total from each camera) may be acquired at 30 frames/sec, by using the on-board memory of the Genesis board.

DGV Software

The software written for both image processing and the operation of the frame grabber is a mixture of C and Visual Basic; see the dissertation by Naylor [12] for a more complete description. VB provides the front-end for all grabbing and processing DLLs, which have been written in C. The acquisition hardware for the reference (photodiode) system is housed in one personal computer, while the frame grabber is installed in a different, nearby PC. Synchronization of the LFMS photodiode and camera based acquisitions for both calibration and velocity data has been accomplished by manually triggering both data acquisition systems simultaneously. Because one field is taken after another for the interlaced cameras $1/60^{th}$ of a second apart, the two fields that make up an interlaced image cannot be used as one velocity image in DGV. Instead, only the first field is captured, and in post-processing, the missing lines in the acquired field are filled in with the average of the pixel values directly above and below the empty line, creating a full frame to be analyzed.

The main goal of the image processing software [12] is to accurately represent the imaged area by better aligning the views of the signal and reference cameras. Most of the steps shown closely follow the comprehensive image processing methods developed at NASA Langley by Meyers [31,32]. In addition to the cell calibrations, several additional images need to be taken before each data run, while the system remains undisturbed. In each case where the target is stationary, several exposures are taken and averaged for each camera. The background image is an image (average of several frames) of the data area without laser illumination, which is subtracted from all data images subsequently taken. The next averaged image is one of a rectangular reference grid of small dots placed in the plane of measurement which is key to the spatial corrections needed for accurate alignment of the signal and reference camera images. This "dot card" image provides reference points for image dewarping via bilinear interpolation.

An averaged image of an illuminated white card is also recorded for the flat field correction of data images. The signal and reference images of the white card go through the same processing steps as do the data images up to the ratio step. After the division of signal and reference images, each channel's white card ratio array is normalized with respect to the average ratio value. The resulting matrix of floating point numbers should, ideally, be equal to 1.0, but spatial imperfections in the imaging system (lenses, beamsplitters, mirrors, and cell ends) will cause variations in the ratio. Ratioed DGV data images are then divided by the white card matrix to correct for these imperfections [31]. In an effort to force all pixels in each CCD array to have the same sensitivity, two average images are taken with all lenses removed and the array exposed to

two different light levels [32]. These images only need to be taken once, since the pixel sensitivity imperfections are inherent to the cameras and are not likely to change with changes to the configuration or alignment of the system. Individual pixel sensitivities (or slopes), which, ideally, should be equal to 1.0, are calculated for each pixel and the correction is applied by dividing the data image from each camera by the corresponding array of pixel slopes [32]. When viewing false color images of the pixel correction images, unique "hot spot" patterns can be seen for each camera which are identical in shape to features seen in the raw data images, reaffirming the need for this type of correction.

The next step in the algorithm is to low-pass filter the image resulting from the steps above. A convolution is performed between a flat 5x5 kernel and the image, in effect, blurring it. Low-pass filtering reduces the effects of both the CCD readout noise, as well as any laser speckle noise [28,29]. Speckle noise is less of a problem with the cw laser used in this research than with a pulsed laser, but low-pass filtering still improves the quality of the images acquired. The MTF of the camera-lens combination has been found to be approximately 5 pixels wide, so a 5x5 kernel actually causes minimal loss of meaningful spatial variations in velocity [12].

Jet Facility

For the present work, the 1" diameter uniform axisymmetric jet flow facility that was used for the point Doppler data has again been utilized; see Fig. 5. This jet is fed from a plenum fitted with a flow-straightening element, via a 16:1 area ratio nozzle. The nozzle has been fitted with an annular centerbody (Fig. 6) to create the annular jet with a low axial velocity on the centerline at the exit [15], or with a swirler to create a swirling jet having an exit swirl number of approximately 0.33. The flow is driven by a variable-speed blower, which can achieve exit velocities of just over 100 m/sec. For the present results, the jet has been run at an exit velocity of nominally 60 m/s, corresponding to a Reynolds number of 100,000. Flow seeding for DGV measurements is provided by a commercial ROSCO fog machine, which feeds a large plenum, to damp out pulsations in smoke output. Also, the amount of smoke produced has been reduced by placing a diode in series with the motor that drives the fog fluid pump.

The computer-controlled, three-axis traversing system developed by Ramanath [18] has been used to position the jet flow facility with respect to the fixed DGV system, so that velocity contours may be mapped out in a series of crossflow planes along the jet axis.

Data Acquisition

Two-component DGV data (axial and circumferential components) have been obtained for the standard jet for a series of cross-flow planes at x/D = 0.5, 1, 2, 3, 4, 5, 6, 9, and 12. Similar data runs are currently under way for the swirling and annular jets. For each jet configuration, multiple runs will be made to assess data repeatability. Single-component constant temperature hot wire anemometer data has previously been acquired for the standard jet and the swirling jet, for comparison with the DGV results. Also, two-component pDv data has been obtained for the three jets [19, 20], again for comparison with the DGV results.

Doppler Global Velocimeter Results

The configuration geometry for the present DGV jet flow measurements is similar to that of the point Doppler velocimeter runs, as has been shown in Fig. 1. One DGV component has been configured in forward scatter, and is primarily sensitive to the jet axial velocity, while the other DGV channel has been operated in back scatter and primarily senses the jet circumferential

velocity. However, the back scatter channel signal strength is much less than that of the forward scatter signal. Camera lens f-numbers have been adjusted to compensate for these differences, so that camera gray levels at the jet exit are nominally 150-200 for both reference cameras. The speed of the blower that feeds the pipe flow apparatus has again been set to a nominal centerline exit velocity of 60 m/sec based on pitot-static probe data, corresponding to an exit Reynolds number of 100,000 based on the jet exit diameter.

Examples of the improved DGV two-component mean axial velocity data for the standard jet are presented in Fig. 22. These data have been reduced as two separate DGV systems, by dividing the measured velocities in the sensitivity directions by the cosine of the angle between the appropriate sensitivity direction and the known flow direction. Here, the velocities have been presented as false color images, where the red color corresponds to 60 m/sec, green corresponds to 30 m/sec, and blue corresponds to 0 m/sec. These new DGV data, obtained using the vapor-limited iodine cells, do not exhibit the mean velocity zero offset error that was seen in the earlier results of Naylor and Kuhlman [4, 12]. These results will be presented in more detail by Kuhlman, Scarberry, and Burton in reference [33].

Conclusions

A two-component point Doppler velocimeter system using iodine vapor absorption cells has been significantly improved in the present work through the use of vapor-limited cells that are not sensitive to temperature variations. Also, use of a smaller measurement volume has improved the RMS results. Two-component velocity measurements have been obtained for a 1 inch diameter uniform circular jet flow at a nominal exit velocity of 60 m/sec, corresponding to a Reynolds number of 100,000. Similar results have been obtained for more complex annular and swirling jet flows. These data runs have been duplicated to judge the repeatability of these measurements, and also have been compared with hot wire anemometer data for the same flow conditions. Point Doppler velocimeter mean velocity results are generally repeatable to within approximately 1-2 m/sec; the RMS velocity results are repeatable to within 1.0 m/sec. Exit profiles of mean axial velocity data generally agree with hot wire anemometer results to within about 2-4 m/sec. However, the RMS velocity results are consistently 20-28% lower than the hot wire results everywhere but at the exit of the standard jet. This is believed to be due in part to spatial averaging for the point Doppler velocimeter results, as well as to the method used to compute the RMS for some of these results. It is also speculated that the actual flow turbulence levels may have been reduced somewhat by the smoke particle seeding used for the point Doppler velocimeter measurements. At the jet exit, the RMS values of 1-1.5 m/sec correspond to about two percent of the exit mean velocity. This resolution is correctly predicted by an error model that propagates the effects of the A/D board resolution on the measured velocity, and is not too different from noise levels typically achieved by conventional LV systems using counter processors. It is believed that further improvements in this minimum velocity resolution should be achievable through use of a better A/D board, along with large-area avalanche photodiodes, to improve the instrument signal-to-noise ratio.

The two-component Doppler Global Velocimeter (DGV) system has also been significantly improved in the present work through the use of the same vapor-limited iodine cells that are not sensitive to temperature variations. Two-component DGV velocity measurements have been obtained for a 1 inch diameter uniform circular jet flow at a nominal exit velocity of 60 m/sec, and similar results are also being obtained for an annular jet and a swirling jet. These DGV data

runs will be duplicated to judge the repeatability of these measurements, and also will be compared with hot wire anemometer data and pDv data for the same flow conditions. PDv mean velocity results using the new iodine cells were repeatable to within approximately 1-2 m/sec; the improved DGV mean velocity results are also repeatable to a similar level.

Acknowledgements

The present work has been supported under AFOSR/DEPSCoR Grants F49620-94-1-0434 and F49620-98-1-0068, Drs. J. M. McMichael, M. Glauser, and T. Beutner, technical monitors. Additional support under NASA Langley Research Center Grants NAG-1-1892 and NAG-1-2132, Mr. James F. Meyers, technical monitor, is acknowledged. The author is grateful for the technical assistance of Jim Meyers, Joe Lee, Rich Schwartz, Angelo Cavone, and Gary Fleming at NASA Langley Research Center, and Bob McKenzie and Mike Reinath at NASA Ames Research Center.

References

1. Komine, H., Brosnan, S. J., Litton, A. B., and Stappaerts, E. A, "Real-Time Doppler Global Velocimetry," paper AIAA-91-0337, AIAA 29th Aerospace Sciences Meeting, Jan. 7-10, 1991, Reno, NV.

2. Kuhlman, J. M., Naylor, S., James, K., and Ramanath, S., "Accuracy Study of a 2 – Component Point Doppler Velocimeter (PDV)," paper AIAA-97-1916, presented at AIAA 28th Fluid Dynamics Conference, June 29-July 2, 1997, Snowmass, CO.

3. Naylor, S. and Kuhlman, J., "Results for a Two-Component Doppler Global Velocimeter (DGV)," paper AIAA-99-0268, AIAA 37th Aerospace Sciences Meeting, Jan. 11-14, 1999, Reno, NV.

4. Naylor, S. and Kuhlman, J., "Results for a Two-Component Doppler Global Velocimeter," AIAA Journal, Vol. 38, No. 5, May, 2000, pp. 835-842.

5. Webb, D. W., "Development of and Measurements using a Point Doppler Velocimetry (PDV) System," MS Thesis, West Virginia University, MAE Department, 1999.

6. Kuhlman, J. M. and Webb, D. L., "2-Component Point Doppler Velocimetry (PDV) Measurements of Turbulent Flow over an Airfoil," paper AIAA-99-3517, presented at AIAA 30th Fluid Dynamics Conference, June 28-July 1, 1999, Norfolk, VA.

7. Elliott, G. S. and Beutner, T. J., "A Review of Recent Advancements in Molecular Filter Based Planar Doppler Velocimetry Systems," Progress in Aerospace Sciences, Vol. 35, 1999, pp. 799-845.

8. Meyers, J. F., Lee, J. W., and Cavone, A. A., "Signal Processing Schemes for Doppler Global Velocimetry," 14th International Congress on Instrumentation in Aerospace Simulation Facilities, Oct. 27-31, 1991, Rockville, MD.

9. James, K., "Determination of the Accuracy of a Two-Component Point Doppler Velocimetry System," MS Thesis, West Virginia University, MAE Department, 1997.

10. Elliott, G. S., Samimy, M., and Arnette, S. A., "Details of a Molecular Filter-Based Velocimetry Technique," paper AIAA - 94-0490, AIAA 32nd Aerospace Sciences Meeting, Jan. 10-13, 1994, Reno, NV.

11. Mosedale, A., Elliott, G. S., Carter, C. D., and Beutner, T. J., "On the Use of Planar Doppler Velocimetry," paper AIAA-98-2809, AIAA 20th Aerodynamic Measurement and Ground Testing Conference, June 15-18, 1998, Albuquerque, NM.

12. Naylor, S., "Development and Accuracy Determination of a Two-Component Doppler

Global Velocimeter (DGV)," PhD Dissertation, West Virginia University, MAE Department, 1998.

13. Wygnanski, I. and Fiedler, H., "Some Measurements in the Self-Preserving Jet," Journal of Fluid Mechanics, Vol. 38, Part 3, 1969, pp. 577-612.

14. Kuhlman, J. M. and Gross, R. W., "Three-Component Velocity Measurements in an Axisymmetric Jet using LDV," DANTEC Information, No. 12, Feb. 1993, pp. 10-16.

15. Kuhlman, J. M., "Variation of Entrainment in Annular Jets," AIAA Journal, Vol. 25, No. 3, March 1987, pp. 373-379.

16. Kuhlman, J. M., "Turbulence Measurements in Annular Jets Using Laser Velocimetry," presented at ASME Symposium on Laser Anemometry: Advances and Applications, June 19-23, 1994, Lake Tahoe, NV.

17. Hussain, H. J., George, W. K., and Capp, S. P., "Comparison between Hot-Wire and Burst-Mode LDA Velocity Measurements in a Fully-Developed Turbulent Jet," paper AIAA-88-0424, presented at AIAA 26th Aerospace Sciences Meeting, Jan. 11-14, 1988, Reno, NV.

18. Ramanath, S., "Development of a Point Doppler Global Velocimeter (DGV)," MS Thesis, West Virginia University, MAE Department, 1997.

19. Collins, P., "Point Doppler Velocimetry (PDV) Measurements in Circular Jets," MS Thesis, West Virginia University, MAE Department, 2000.

20. Kuhlman, J. and Collins, P., "Circular Jet 2-Component Point Doppler Velocimetry (PDV) Velocity Data," paper AIAA-2000-2296, presented at AIAA 21st Aerodynamic Measurement Technology and Ground Testing Conference, June 19-22, 2000, Denver, CO.

21. Kuhlman, J. and Scarberry, T., "Improved Point Doppler Velocimeter (pDv) Turbulence Data in Circular Jets," paper AIAA-2001-0700, presented at AIAA 39th Aerospace Sciences Meeting, Jan. 8-11, 2001, Reno, NV

22. Kuhlman, J., Collins, P. and Scarberry, T., "Two-component point Doppler velocimetry data in circular jets," Measurement Science and Technology, Vol. 12, No. 4, April 2001, pp. 395-408.

23. Kuhlman, J., "Development of Doppler Global Velocimeter," Final Report for AFOSR/DEPSCoR Grant F49620-94-1-0434, May, 1998.

24. Laufer, J., "The Structure of Turbulence in Fully Developed Pipe Flow," NACA TR 1174, 1954.

25. Forkey, J.N., Finklestein, N.D., Lempert, W.R., and Miles, R. B., "Control of Experimental Uncertainties in Filtered Rayleigh Scattering Measurements," paper AIAA-95-0298, presented at AIAA 33rd Aerospace Sciences Meeting, Jan. 9-12, 1995, Reno, NV; also AIAA Journal, Vol. 34, No.3, Mar. 1996, pp. 442-448.

26. Thorpe, S. J., Ainsworth, R. W., and Manners, R. J., "Time-Averaged Free-Jet Measurements Using Doppler Global Velocimetry," ASME Fluids Engineering Div. Conf., FED-Vol. 239, Volume 4, 1996.

27. Longmire, E. K. and Eaton, J. K., "Structure and Control of a Particle-Laden Jet," Report No. MD-58, Dept. of Mechanical Engineering, Stanford Univ., Stanford, CA, Sept. 1990.

28. McKenzie, R. L., "Planar Doppler Velocimetry Performance in Low-Speed Flows," paper AIAA-97-0498, AIAA 35th Aerospace Sciences Meeting, Jan. 6-10, 1997, Reno, NV.

29. Smith, M. W., "The Reduction of Laser Speckle Noise in Planar Doppler Velocimetry Systems," paper AIAA-98-2607, AIAA 20th Aerodynamic Measurement Technology and Ground Testing Conference, June 15-18, 1998, Albuquerque, NM.

30. Kuhlman, J. M., "Test Performance of WVU Two - Component Point Doppler

Velocimeter (PDV) System," Final Report to Metrolaser, Inc., of Irvine, Ca, November, 2000.

31. Meyers, J. F., "Evolution of Doppler Global Velocimetry Data Processing," 8th Int'l. Symp. On Applications of Laser Techniques to Fluid Mechanics, July 8-11, 1996, Lisbon, Portugal.

32. Meyers, J. F., "Doppler Global Velocimetry, The Next Generation?," paper AIAA-92-3897, presented at AIAA 17th Ground Testing Conference, July 6-8, 1992, Nashville TN.

33. Kuhlman, J., Scarberry, T., and Burton, L., "Doppler Global Velocimetry (DGV) Data in Circular Jets," paper 7.3, 19th International Congress on Instrumentation in Aerospace Simulation Facilities, August 27-30, 2001, Cleveland, OH.

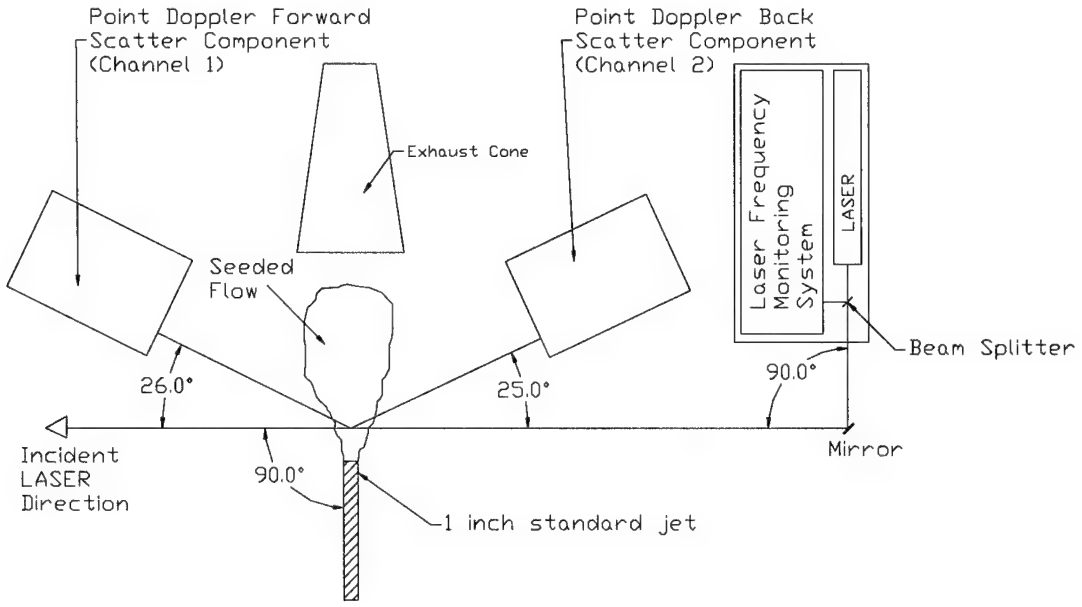

Fig. 1 Schematic of point Doppler velocimeter system configuration

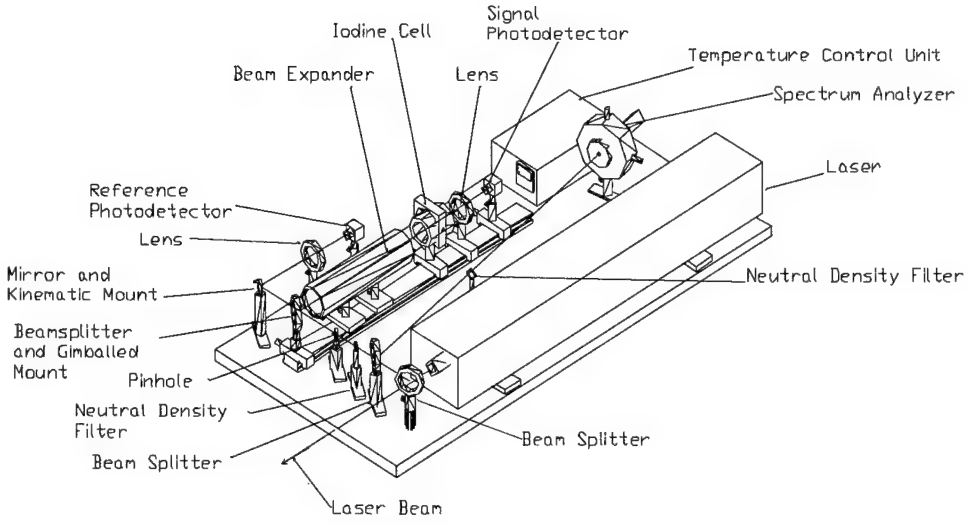

Fig. 2 Laser frequency monitoring system, laser, and spectrum analyzer

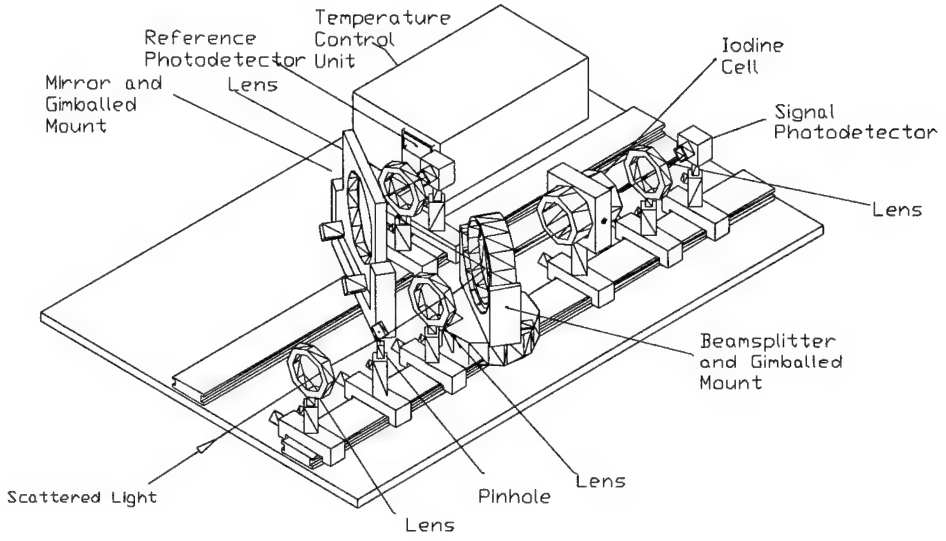

Fig. 3 Schematic of one of two point Doppler velocimeter components

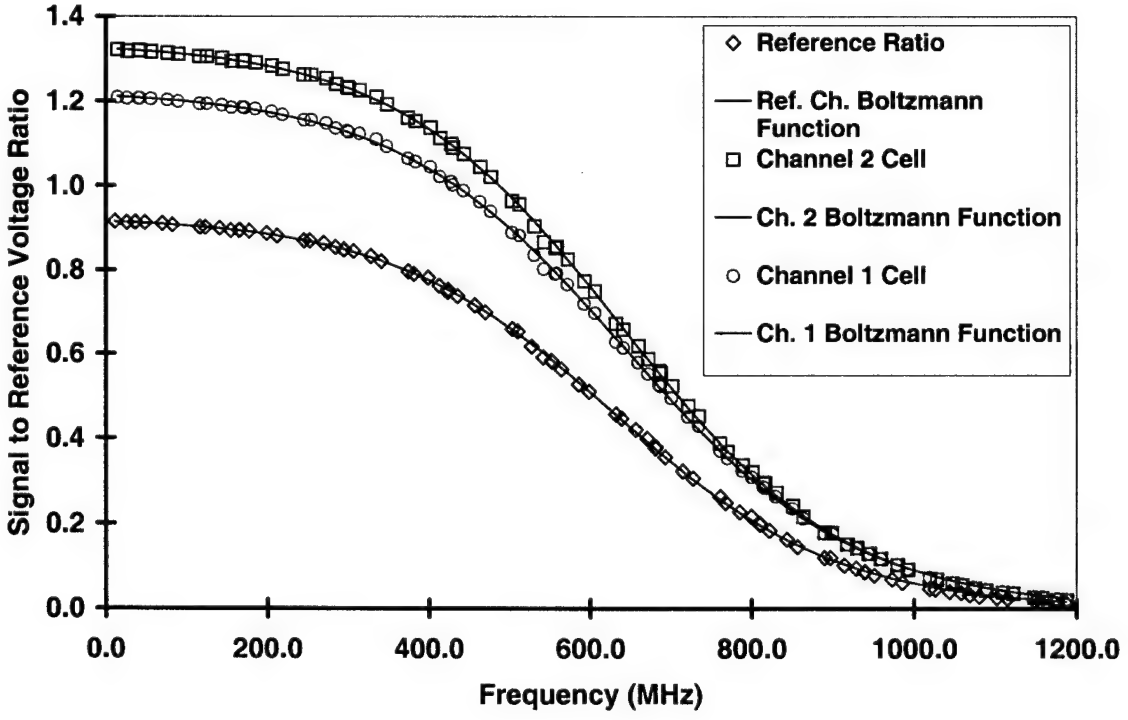

Fig. 4 Example of iodine cell calibrations and Boltzmann function curve fits

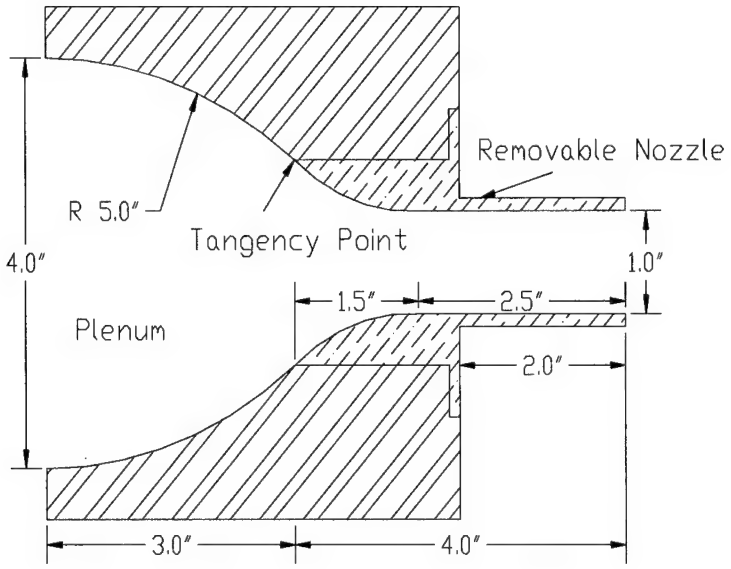

Fig. 5 Standard jet nozzle and plenum

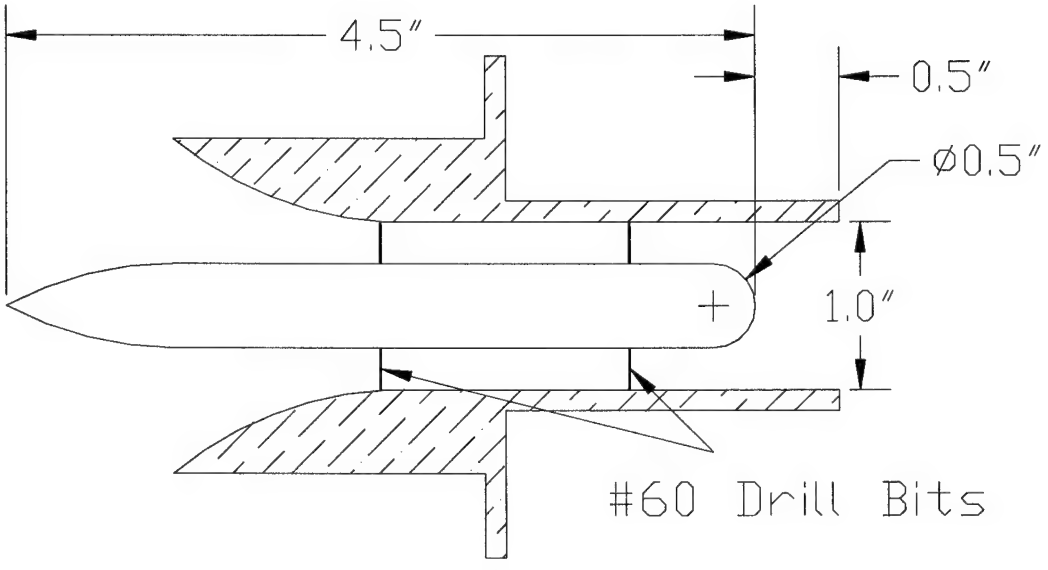

Fig. 6 Annular nozzle and centerbody

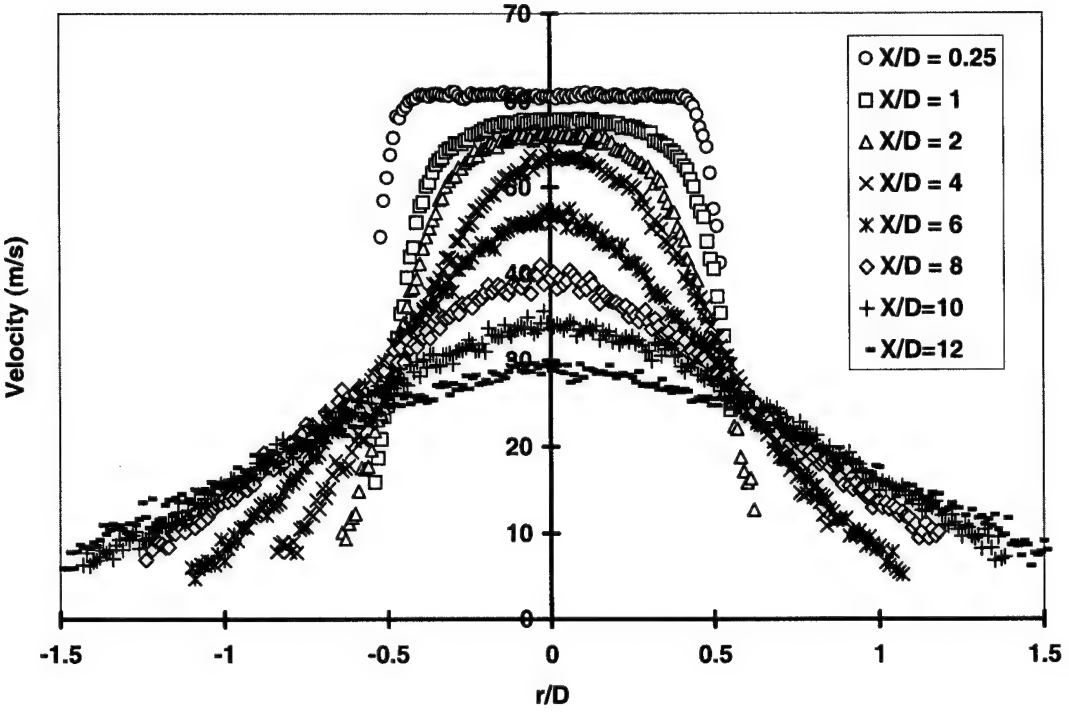

Fig. 7 Composite plot of axial mean velocities for standard jet; run 2

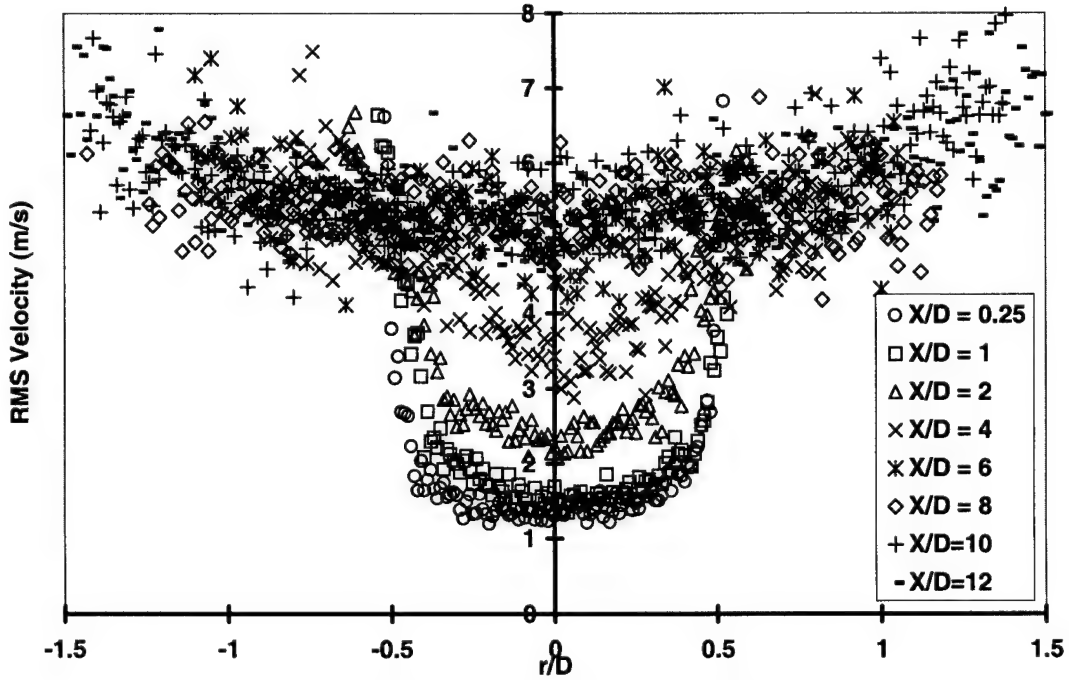

Fig. 8 Composite plot of axial RMS velocities for standard jet; run 2

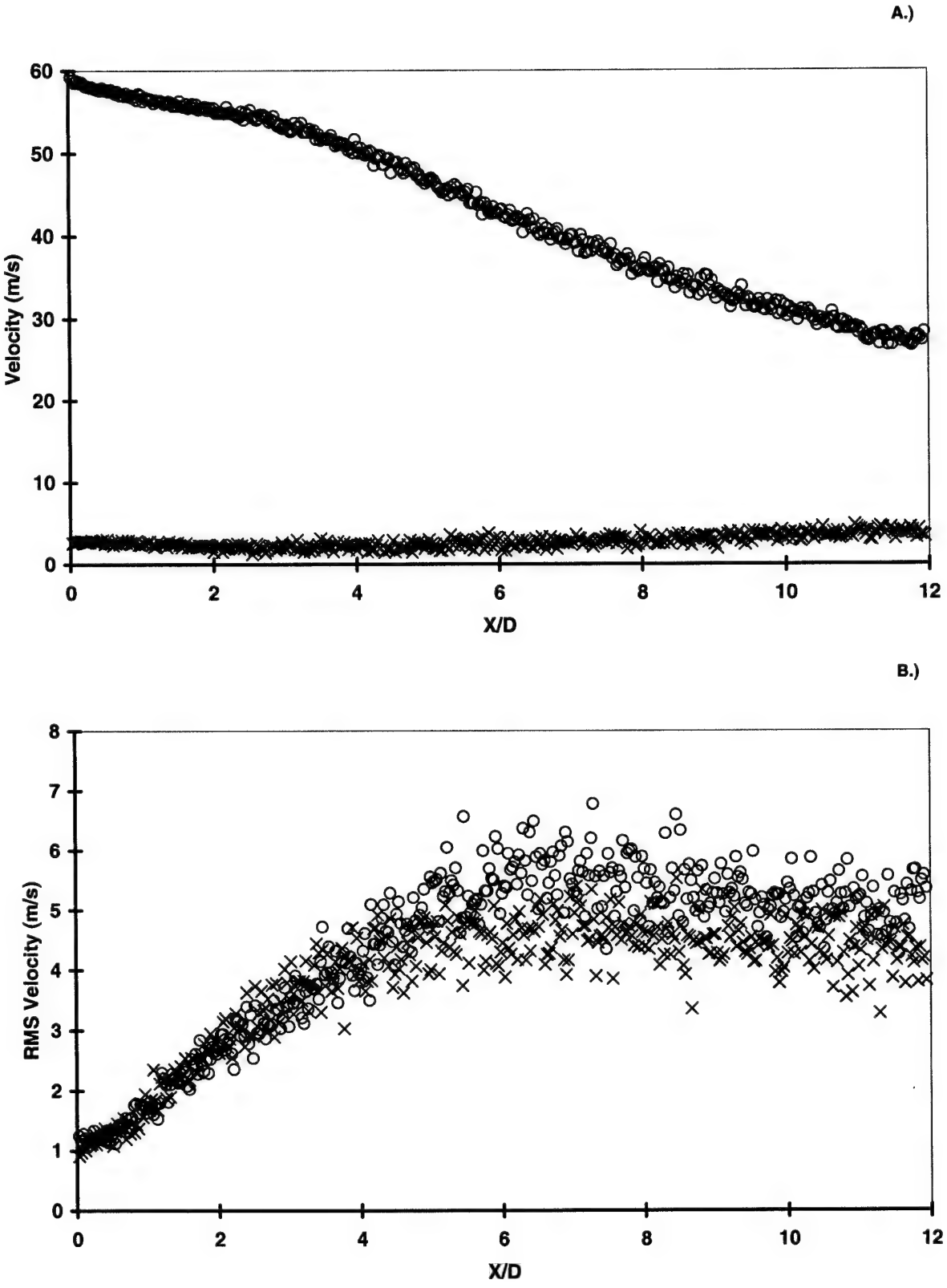

Fig. 9 2-Component velocity results for standard jet centerline; Circles-axial velocity; X's-circumferential velocity

a.) mean velocities

b.) RMS velocities

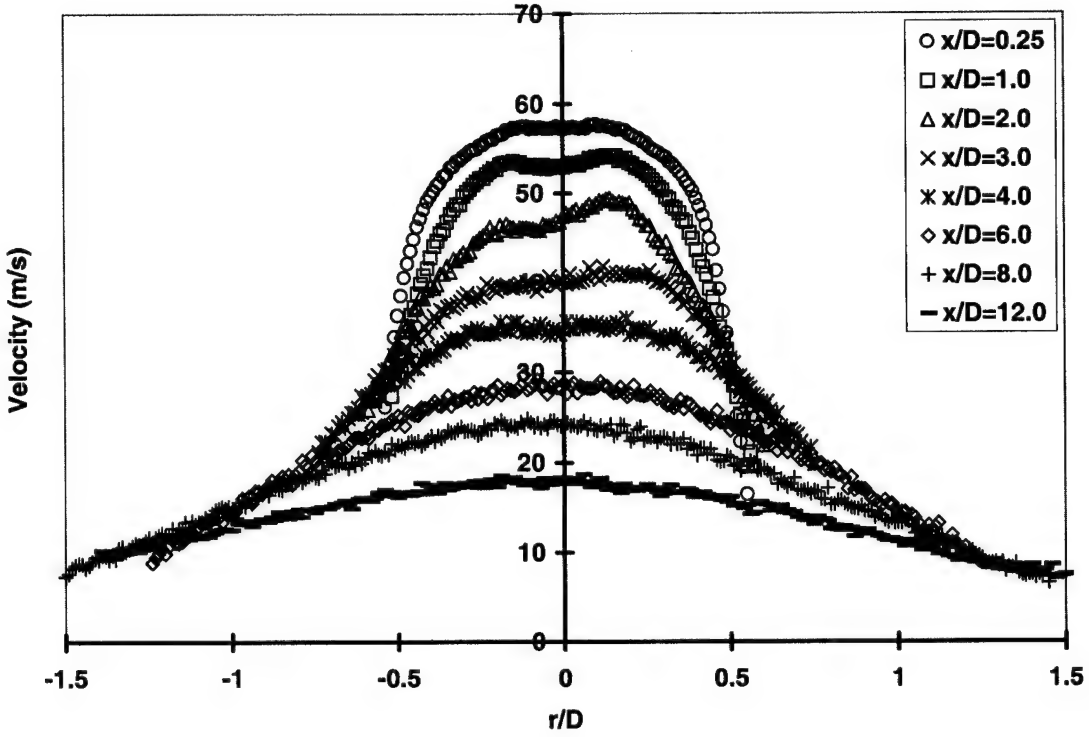

Fig. 10 Composite plot of axial mean velocities for swirling jet; run 1

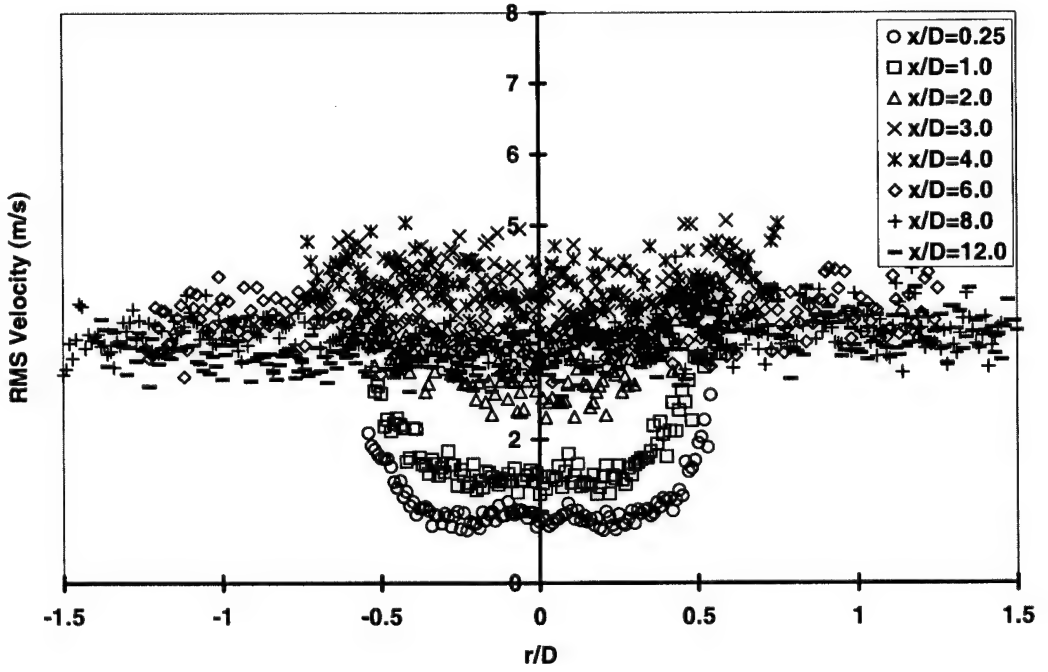

Fig. 11 Composite plot of axial RMS velocities for swirling jet; run 1

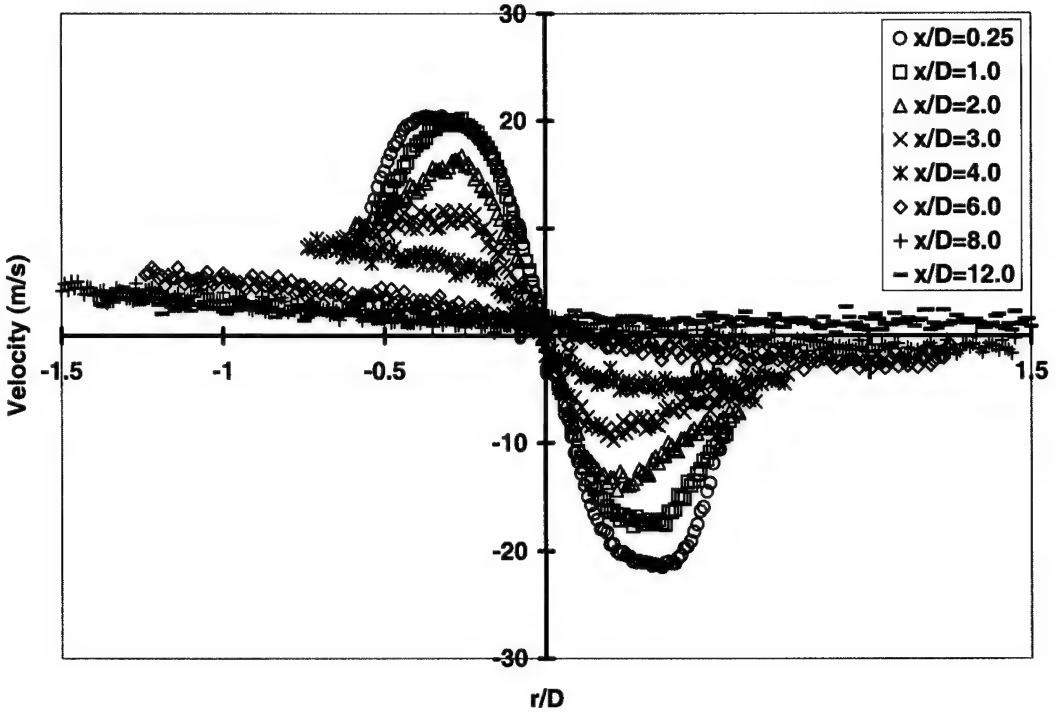

Fig. 12 Composite plot of circumferential mean velocities for swirling jet; run 1

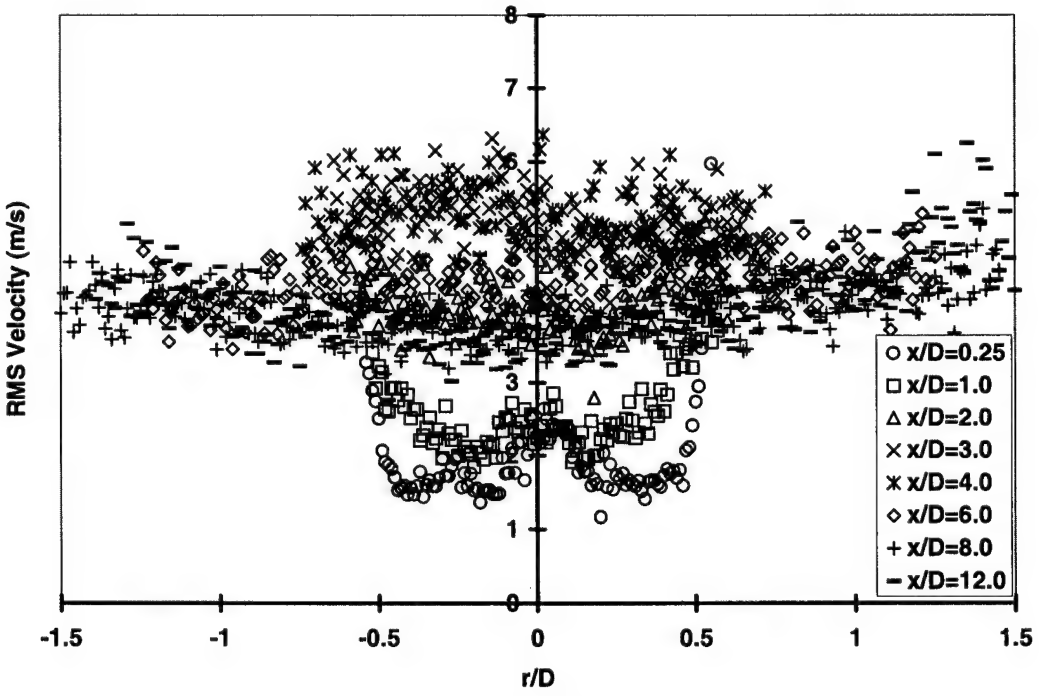

Fig. 13 Composite plot of circumferential RMS velocities for swirling jet; run 1

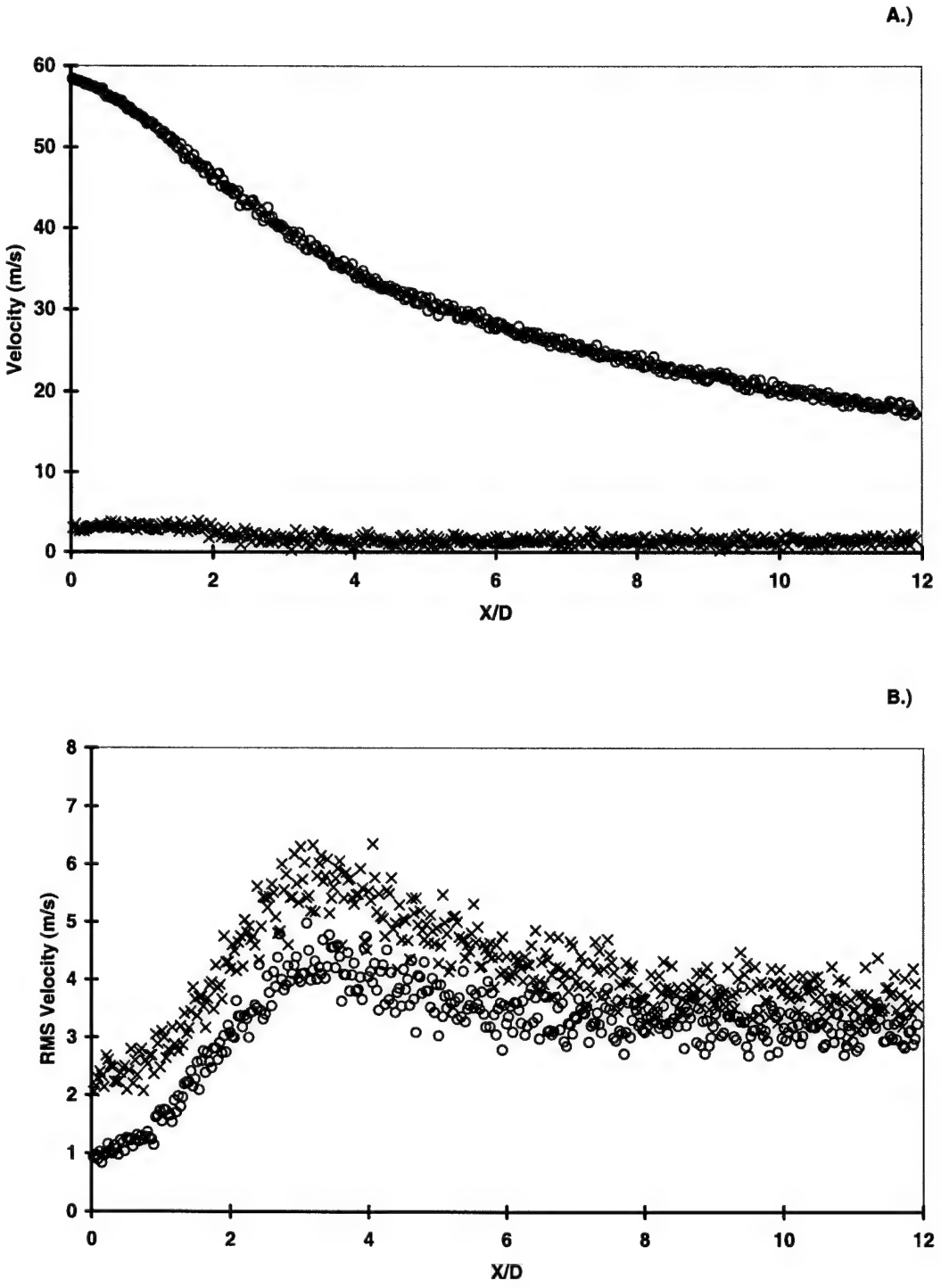

Fig. 14 2-Component velocity results for swirling jet centerline; Circles-axial velocity; X's-circumferential velocity

a.) mean velocities

b.) RMS velocities

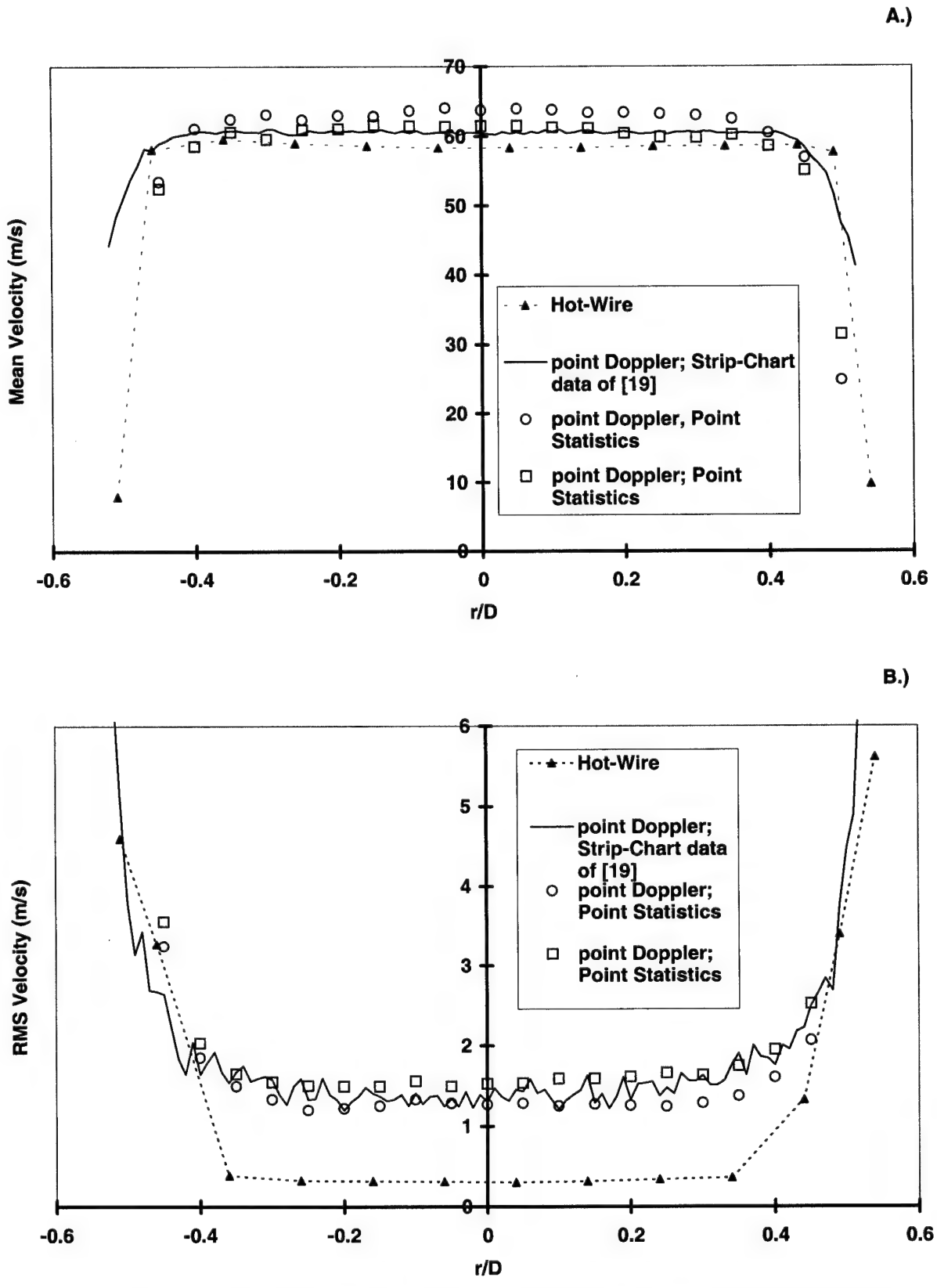

Fig. 15 Comparison of point Doppler velocimeter and hot wire results; standard jet - axial velocities at exit (x/D = 0.25)

a.) mean velocities

b.) RMS velocities

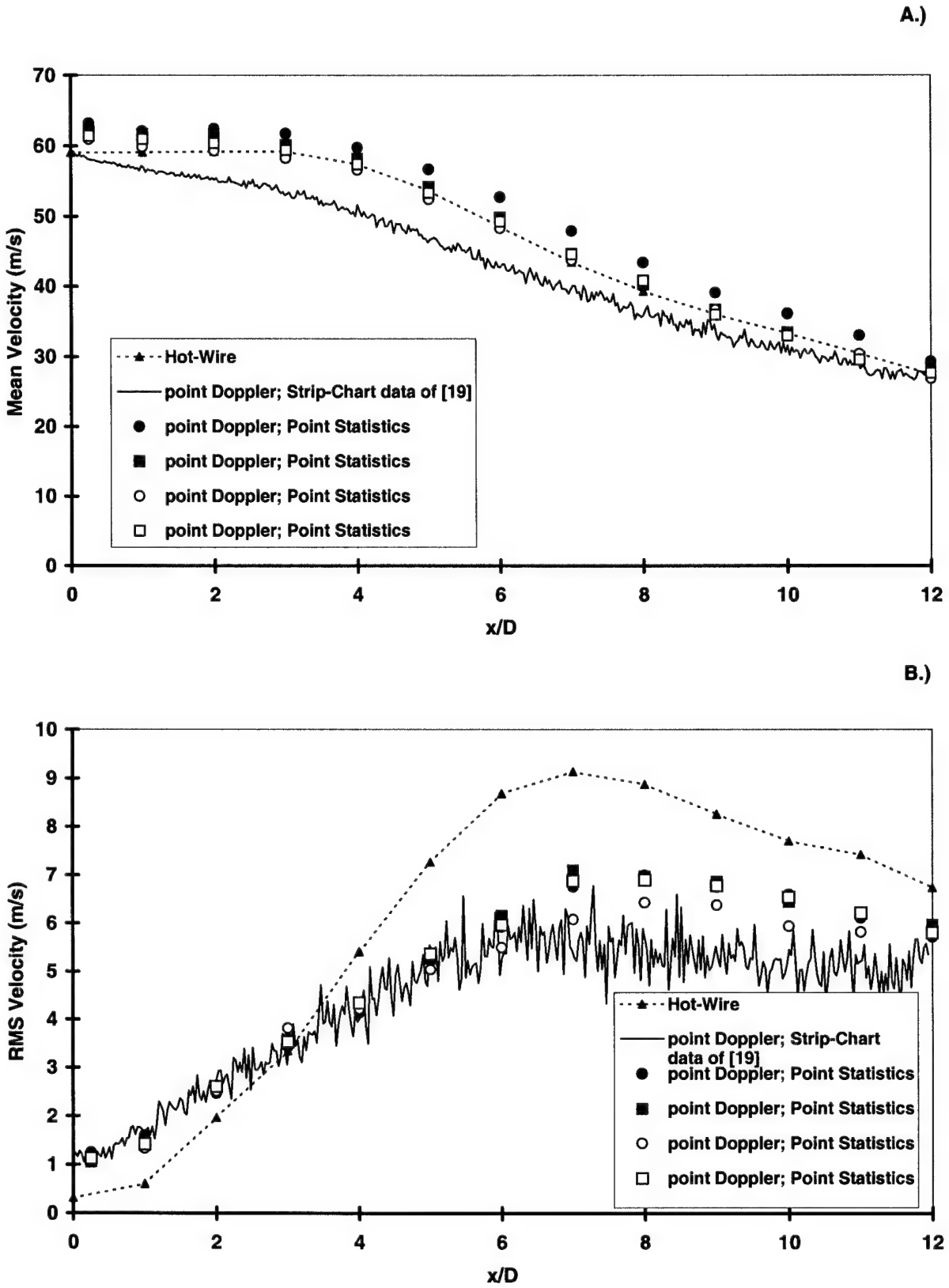

Fig. 16 Comparison of point Doppler velocimeter and hot wire results: standard jet – axial velocities along centerline

a.) mean velocities

b.) RMS velocities

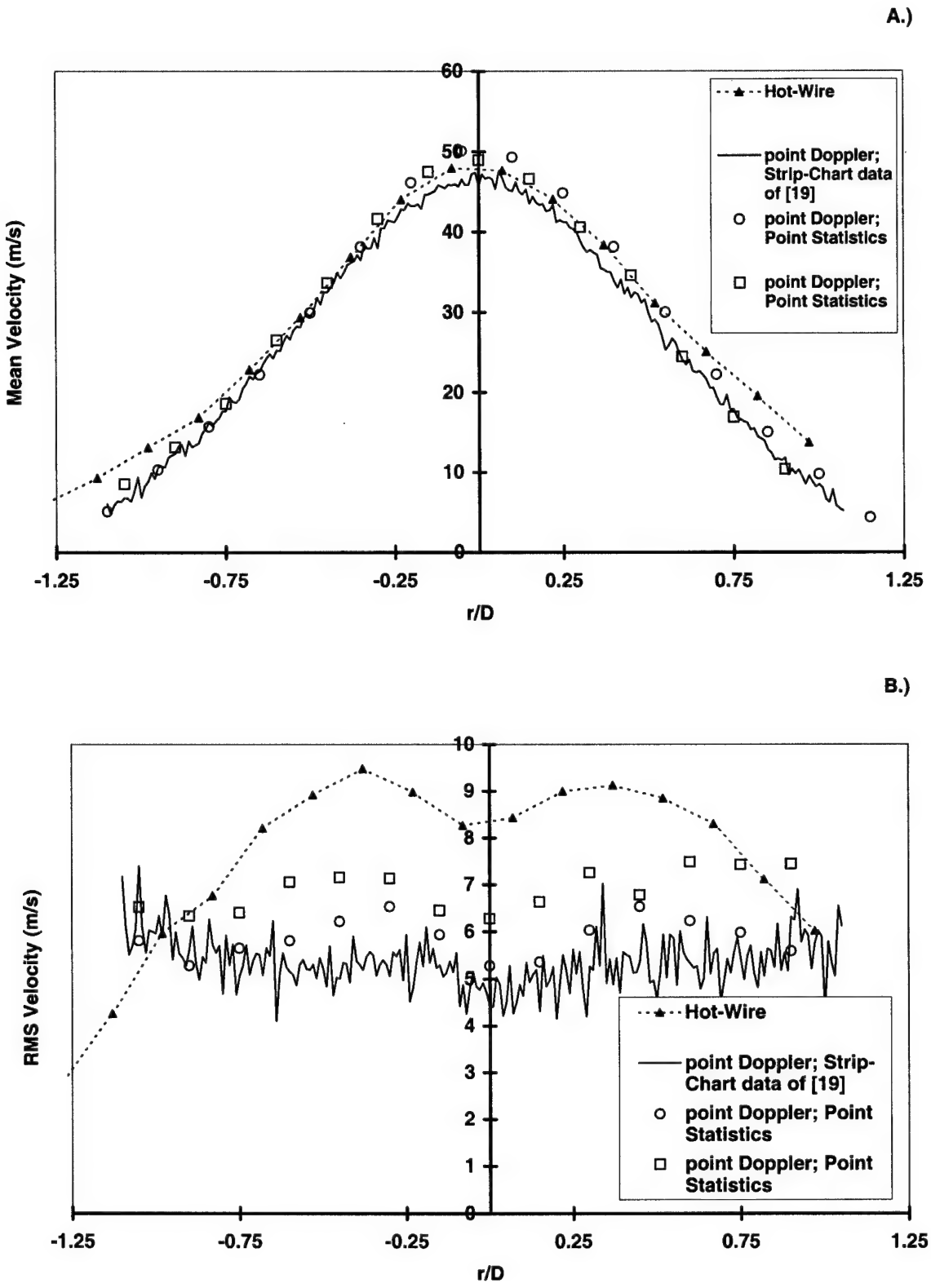

Fig. 17 Comparison of point Doppler velocimeter and hot wire results: standard jet – axial velocities at x/D = 6

a.) mean velocities

b.) RMS velocities

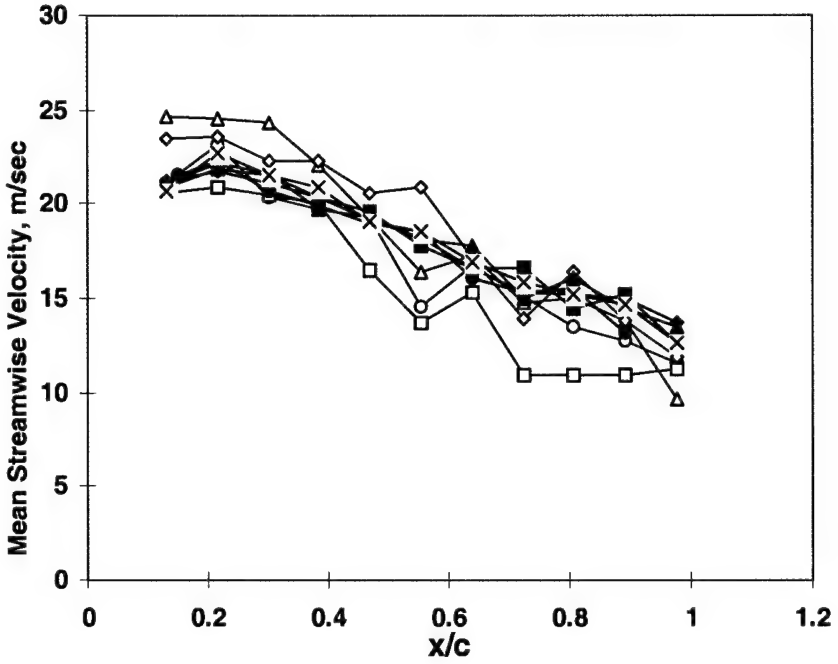

Fig. 18 Comparison of PDV and hot wire streamwise mean velocity over airfoil [6] (open symbols-PDV, filled symbols-HW)

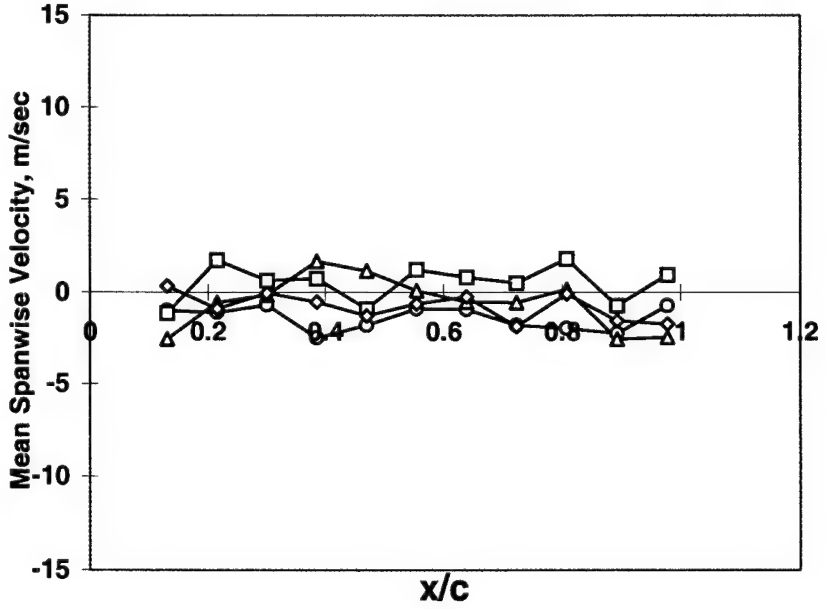

Fig. 19 PDV spanwise mean velocity over airfoil [6] (open symbols-PDV)

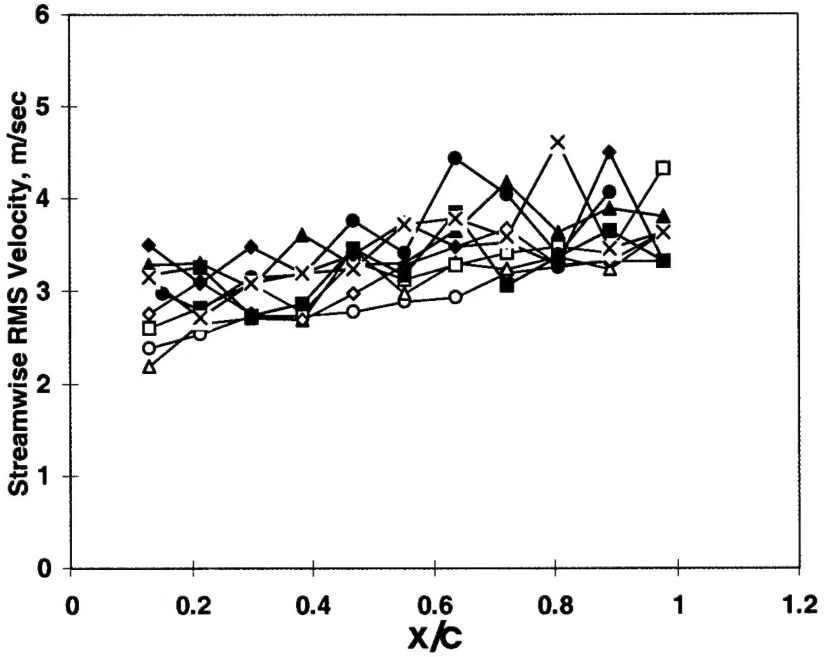

Fig. 20 Comparison of PDV and hot wire streamwise RMS velocity over airfoil [6] (open symbols-PDV, filled symbols-HW)

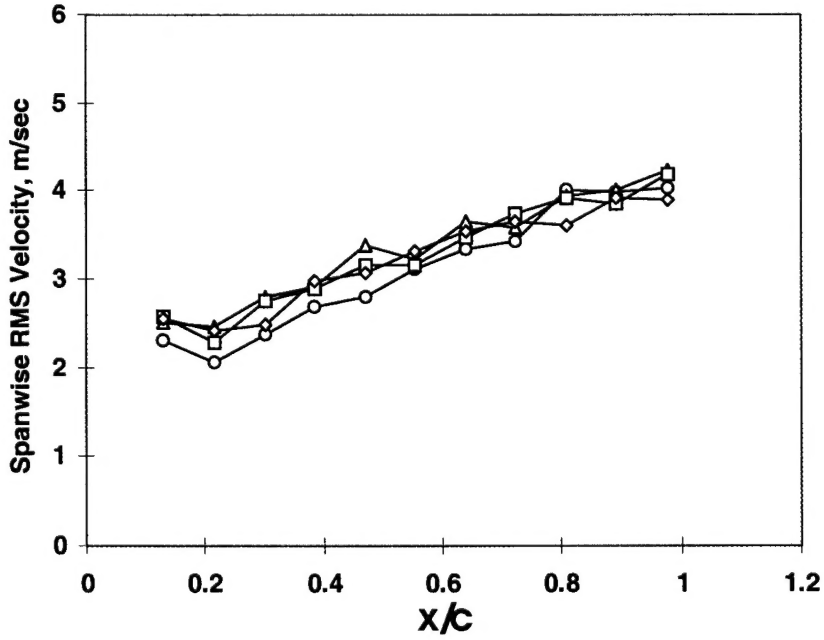

Fig. 21 PDV spanwise RMS velocity over airfoil [6] (open symbols-PDV)

Back Scatter Channel x/D = 0.5 Forward Scatter Channel

Back Scatter Channel x/D = 1.0 Forward Scatter Channel

Back Scatter Channel x/D = 2.0 Forward Scatter Channel

Fig. 22 2-Component DGV mean axial velocity results for standard jet: exit velocity = 60 m/sec. (Red = 60 m/sec; Green = 30 m/sec; Blue = 0 m/sec)

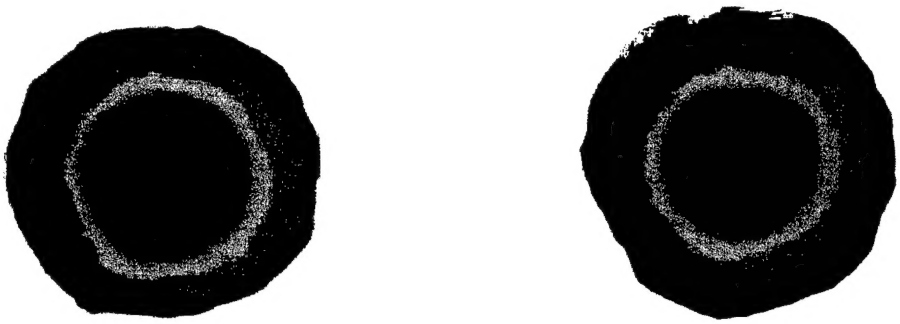

Back Scatter Channel x/D = 3.0 Forward Scatter Channel

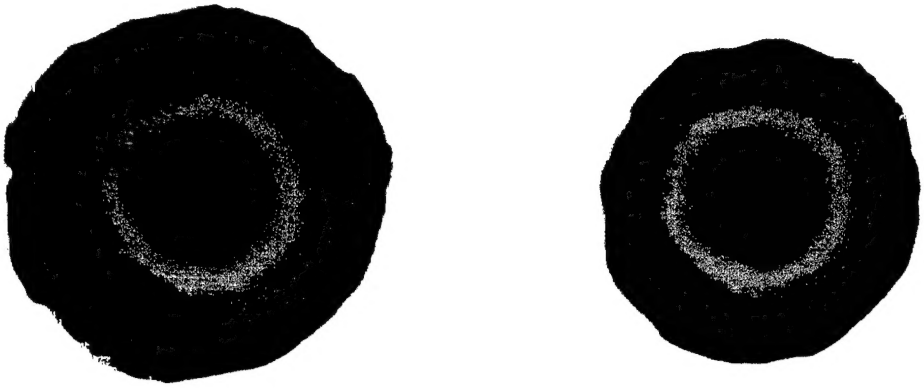

Back Scatter Channel x/D = 4.0 Forward Scatter Channel

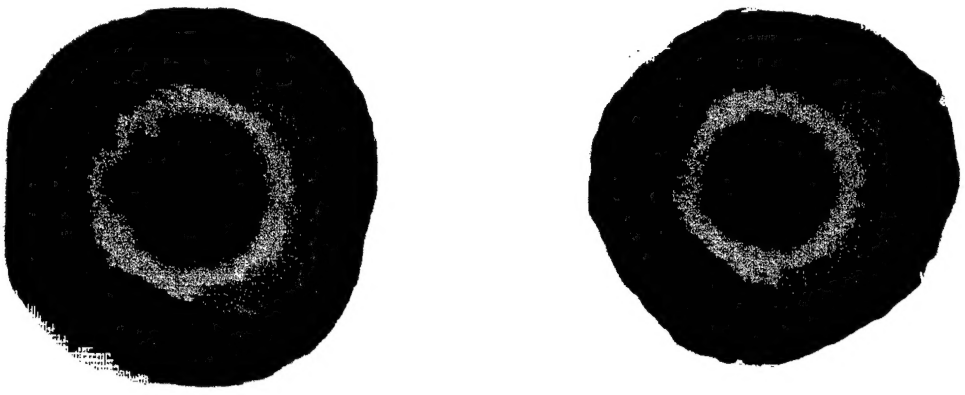

Back Scatter Channel x/D = 5.0 Forward Scatter Channel

Fig. 22(Cont'd.) 2-Component DGV mean axial velocity results for standard jet: exit velocity = 60 m/sec. (Red = 60 m/sec; Green = 30 m/sec; Blue = 0 m/sec)

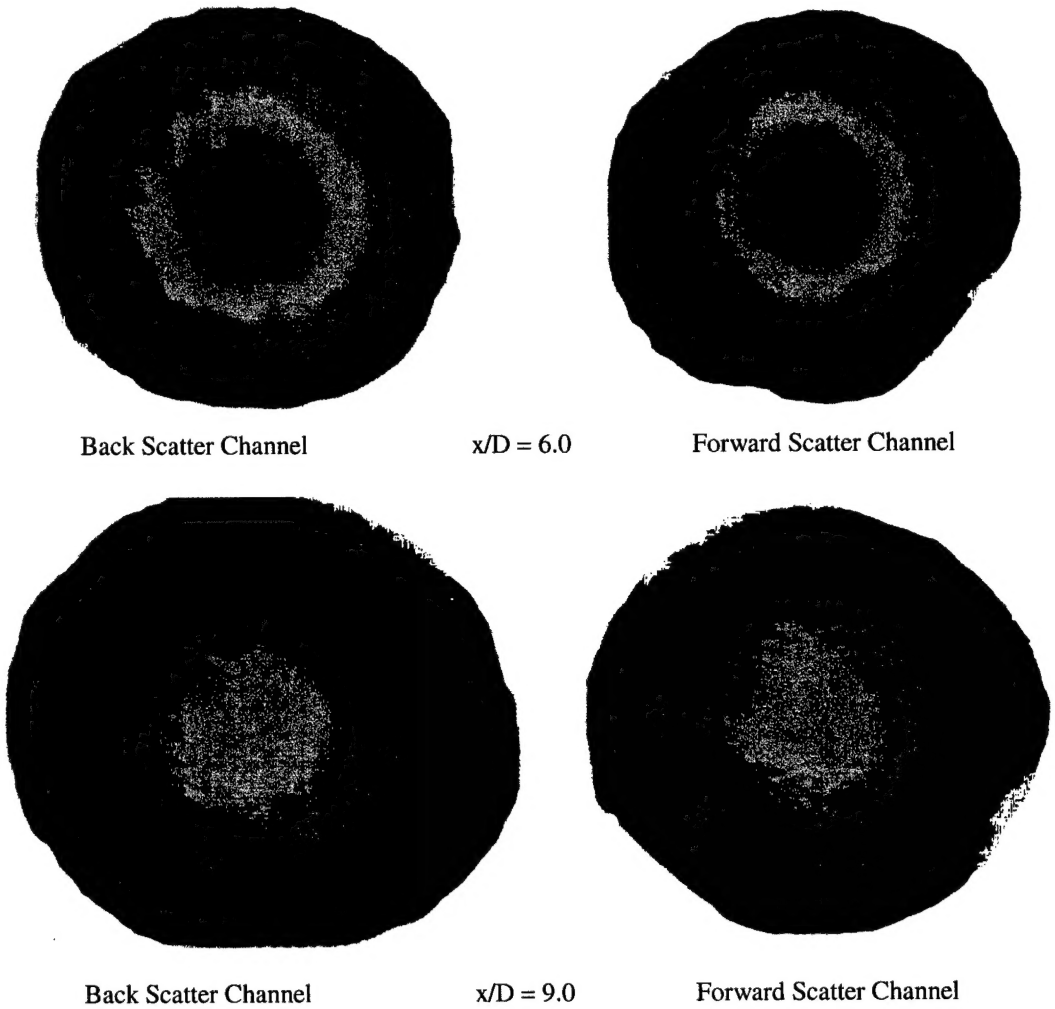

Fig. 22(Concluded) 2-Component DGV mean axial velocity results for standard jet: exit velocity = 60 m/sec. (Red = 60 m/sec; Green = 30 m/sec; Blue = 0 m/sec)